

Journal Pre-proof

The Discovery of Potent Small Molecule Activators of Human STING

David C. Pryde, Sandip Middy, Monali Banerjee, Ritesh Shrivastava, Sourav Basu, Rajib Ghosh, Dharmendra B. Yadav, Arjun Surya



PII: S0223-5234(20)30841-2

DOI: <https://doi.org/10.1016/j.ejmech.2020.112869>

Reference: EJMECH 112869

To appear in: *European Journal of Medicinal Chemistry*

Received Date: 14 July 2020

Revised Date: 21 September 2020

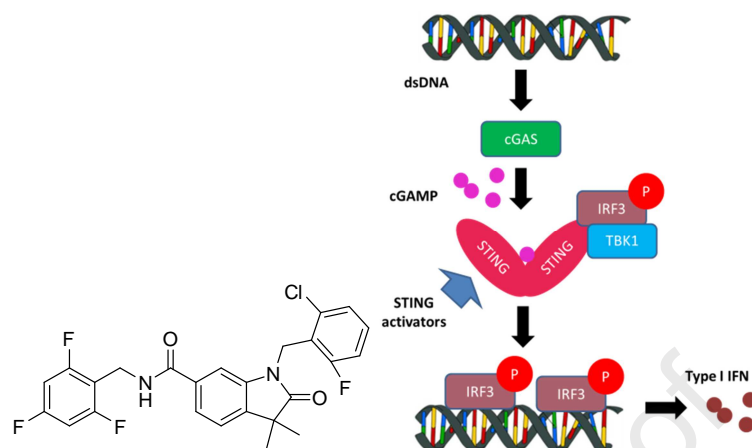
Accepted Date: 21 September 2020

Please cite this article as: D.C. Pryde, S. Middy, M. Banerjee, R. Shrivastava, S. Basu, R. Ghosh, D.B. Yadav, A. Surya, The Discovery of Potent Small Molecule Activators of Human STING, *European Journal of Medicinal Chemistry*, <https://doi.org/10.1016/j.ejmech.2020.112869>.

This is a PDF file of an article that has undergone enhancements after acceptance, such as the addition of a cover page and metadata, and formatting for readability, but it is not yet the definitive version of record. This version will undergo additional copyediting, typesetting and review before it is published in its final form, but we are providing this version to give early visibility of the article. Please note that, during the production process, errors may be discovered which could affect the content, and all legal disclaimers that apply to the journal pertain.

© 2020 Elsevier Masson SAS. All rights reserved.

Graphical abstract



The Discovery of Potent Small Molecule Activators of Human STING

David C. Pryde^{1,}, Sandip Middy², Monali Banerjee², Ritesh Shrivastava², Sourav Basu², Rajib Ghosh², Dharmendra B. Yadav², Arjun Surya²*

¹Curadev Pharma Ltd., Innovation House, Discovery Park, Ramsgate Road, Sandwich, Kent, CT13 9ND, UK. ²Curadev Pharma Pvt. Ltd., B-87, Sector 83, Noida 201305, Uttar Pradesh, India

Keywords

STING, interferon genes, immunotherapy, cytokines.

Corresponding Author

*David C. Pryde, Curadev Pharma Ltd., Innovation House, Discovery Park, Ramsgate Road, Sandwich, Kent, CT13 9ND david@curadev.co.uk.

Abstract

The adaptor protein STING plays a major role in innate immune sensing of cytosolic nucleic acids, by triggering a robust interferon response. Despite the importance of this protein as a potential therapeutic target for serious unmet medical conditions including cancer and infectious disease there remains a paucity of STING ligands. Starting with a benzothiazinone series of

weak STING activators (human EC₅₀ ~10 μM) we identified several chemotypes with sub-micromolar STING activity across all the major protein polymorphs. An example compound **53** based on an oxindole core structure demonstrated robust on-target functional activation of STING (human EC₅₀ 185 nM) in immortalised and primary cells and a cytokine induction fingerprint consistent with STING activation. Our study has identified several related series of potent small molecule human STING activators with potential to be developed as immunomodulatory therapeutics.

1. Introduction

Immunotherapy is a rapidly advancing field, in which the immune system is harnessed and directed towards pathogens and malignancies or towards enhanced vaccine performance [1]. For example, interferon-based regimens have been a mainstay of hepatitis C antiviral therapy for many years while antibodies to inhibitory immune checkpoints such as CTLA-4 and PD-1 have shown considerable promise in treating cancers [2].

The human immune system has evolved to recognize and respond to different types of threats and pathogens to maintain a healthy host [3]. The innate arm of the immune system is mainly responsible for a rapid initial inflammatory response to danger signals associated with cellular or tissue damage from bacteria, viruses and other infectious threats via a number of factors such as cytokines, chemokines and complement factors. An immune response is typically triggered by a pathogen associated molecular pattern (PAMP) (or DAMP, damage associated molecular pattern) [4] binding to a component of the immune system called a Pattern Recognition Receptor (PRR). PRRs include Toll-Like Receptors [5] (TLRs), C-type lectin receptors, retinoic acid

inducible gene I (RIG-I like receptors) [6], NOD-like receptors (NLRs) and double stranded DNA sensors [7].

The protein TMEM173/STING (STimulator of INterferon Genes) has been shown to play a central role in the innate immune response to nucleic acids [8]. Free cytosolic nucleic acids (DNA and RNA) are known PAMPs/DAMPs. The main sensor for cytosolic dsDNA is cGAS (cyclic GMP-AMP synthase) [9] which upon recognition of cytosolic dsDNA, triggers formation of cyclic dinucleotides (CDNs). CDNs are second messenger signalling molecules produced by diverse bacteria and consist of two ribonucleotides that are connected via phosphodiester bonds to make a cyclic structure. CDNs cyclo-di(GMP) (c-diGMP), cyclo-di(AMP) (c-diAMP) and hybrid cyclo-(AMP/GMP) (cGAMP) derivatives all bind strongly to the ER-transmembrane adaptor protein STING [10] to induce a conformational change and generate an active protein state. Activated STING then translocates from the ER to the Golgi, where it can be phosphorylated by TBK1 or IKK kinases to form the STING signalosome and undergo palmitoylation and full activation. The activated signalosome can then phosphorylate IRF3 directly or lead to indirect activation of NF κ B, to aid transcription of cytokines and type-I interferons.

It has been shown that activation of STING increases T cell infiltration into cold or non-inflamed tumors leading to significant regression [11]. The ability of STING activators to generate anti-tumor immune responses in cold tumors in murine models makes them a promising therapeutic option either as a single agent or in combination with existing or developing therapies.

STING activators described in the literature fall into two classes – cyclic dinucleotide (CDN) based and non-CDN small molecules. Currently, the most clinically advanced chemotype

reported is the CDN class derived from the natural ligand structure, which is represented in Phase 1 clinical trials by ADU-S100 [15] (Aduro Biotech/Novartis, **1**, **Figure 1**) and MK-1474 [16] (Merck, structure not disclosed). The CDN class of compounds usually show activity across STING species. Their physicochemical properties are determined by their nucleotide structure and synthesis challenges are common for these multi-chiral center macrocyclic compounds.

The small molecule DMXAA **2** (5,6-dimethylxanthenone-4-acetic acid) has demonstrated immune modulatory activity and disruption of tumor vascularization in a mouse model but failed human clinical trials [12]. Subsequently DMXAA [13], and a related acridinone CMA [14]), was shown to be a potent activator of murine STING but not human STING [14].

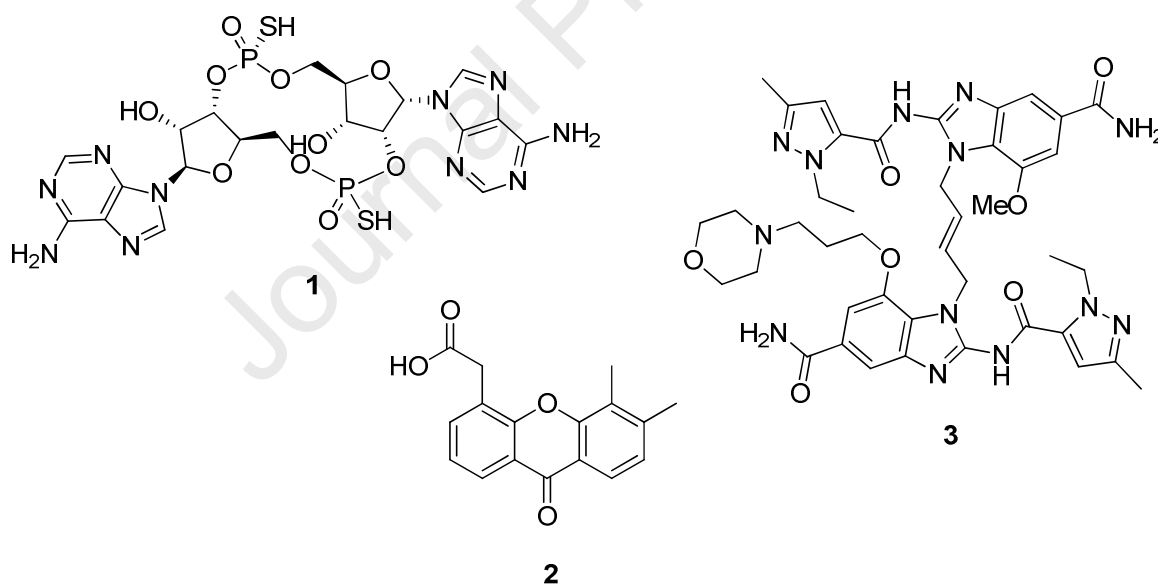


Figure 1. Selected published STING activators

Other reports in the journal and patent literature have described nucleic acid-derived series [17] and some small molecule activators [18-20] including a recent report of ‘dimeric’

benzimidazole derivatives (*e.g.* **3**) from a group at GSK [21], all with varying levels of potency as STING activators.

Several groups have solved the crystal structure of truncated STING in its apo form, as well as bound with ligands [22,8b] and a recent cryo-EM structure of the STING dimer bound to TBK1 [23]. STING forms a symmetrical dimer in apo and ligand-bound states, with all the reported structures so far showing ligands bound in a pocket at the dimer interface and anchored by a network of hydrogen bonds. Interestingly, the STING dimer binds one copy of CDN ligands and the larger ‘dimeric’ class of small molecule, but two copies of the smaller xanthenone/acridinone ligands. Human and mouse STING are 68% identical [24], though the human protein has several naturally occurring variant alleles. Five major haplotypes of human STING have been reported that represent almost 99% of the human population (R232, H232, HAQ, AQ and Q) [25]. One of the challenges with pharmacological intervention in STING signalling is to reliably achieve high potency across all major polymorphisms, with the HAQ polymorphism a particular challenge [26].

Given the importance of STING as a pharmacological target and the limited number of active small molecule chemotypes reported, we initiated a medicinal chemistry program to seek activators of the protein. At the outset of our program, we sought to identify a traditional small molecule drug-like lead series to differentiate it from the natural CDN ligands. We have recently described our early work on a series of benzothiazinones in which weak leads with little or no activity at the HAQ polymorphism (*e.g.* **4**) were developed into potent pan-isoform active compounds *e.g.* **5** through optimisation of peripheral substitution (**Figure 2**) [27].

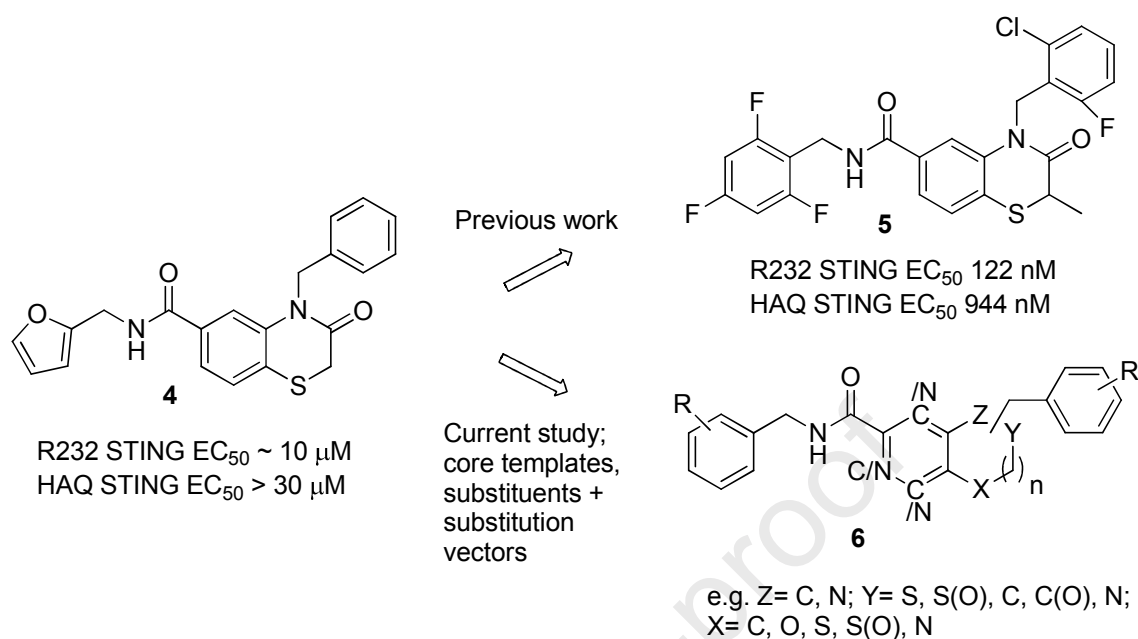


Figure 2. Design strategy. Previous work explored peripheral substitution to improve potency within the benzothiazinone chemotype [27]. The current work sought new core templates to further optimize potency and properties.

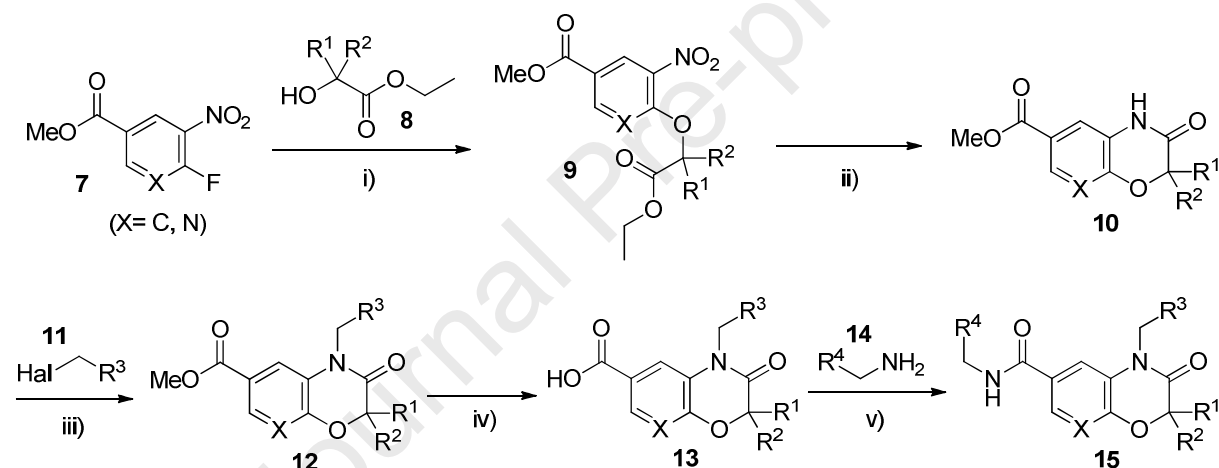
In this manuscript, we describe the medicinal chemistry study that was undertaken to explore several new chemotypes based on the general target structure **6** through modification and optimization of the central core template. Through this effort, we wished to probe the effect of different core ring sizes, heteroatom composition and substitution vectors on STING and its isoforms to ultimately identify suitable potent tool compounds to explore the STING mechanism more fully.

2. Results and Discussion

2.1 Chemistry

The compounds described in the present study were prepared using a variety of straightforward, robust methods. These are described in detail in the Supplementary Material. Illustrative example synthetic schemes are shown below for three different core templates.

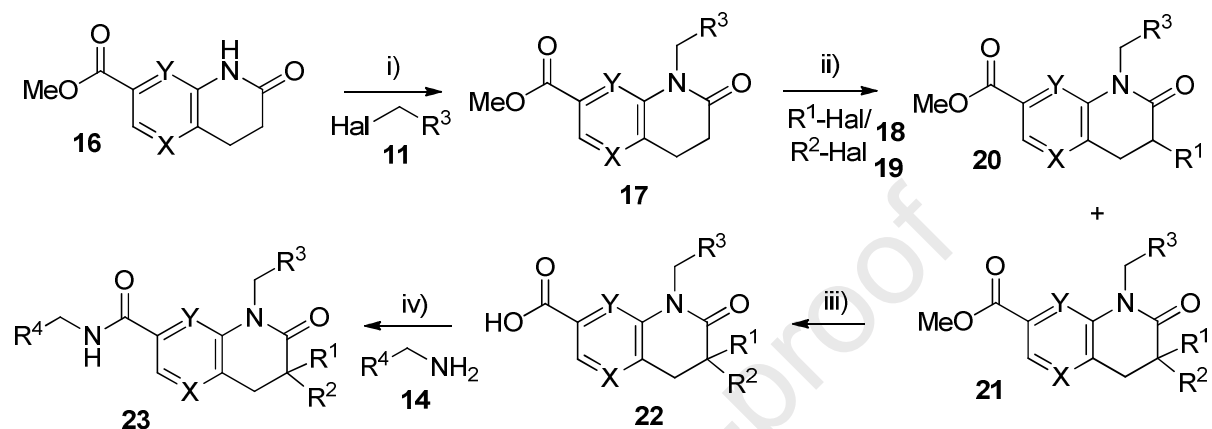
The benzoxazinone core was built starting from a halo-nitro-ester **7** (**Scheme 1**). Halide displacement with a hydroxyester **8** gave the nitro-ether **9**, which upon nitro group reduction and concomitant ring closure gave the fused oxazinone skeleton **10**. Core alkylation with a suitable halide **11** gave the core derivative **12**. Ester hydrolysis and amide coupling to the corresponding acid **13** with a requisite amine **14** gave the final test compound structures **15**.



Scheme 1. Synthesis of benzoxazinones. Reagents and conditions: i) Acetonitrile, triethylamine, 0-5°C, 81-99%; ii) Fe, AcOH, 80°C, 95-99%; iii) 1,2-dichloroethane, NaOH, water, tetrabutylammonium bromide, room temperature, 61-89%; iv) MeOH, water, THF, LiOH.H₂O, room temperature, 74-99%; v) DMF, HATU, triethylamine, room temperature, 20-84%.

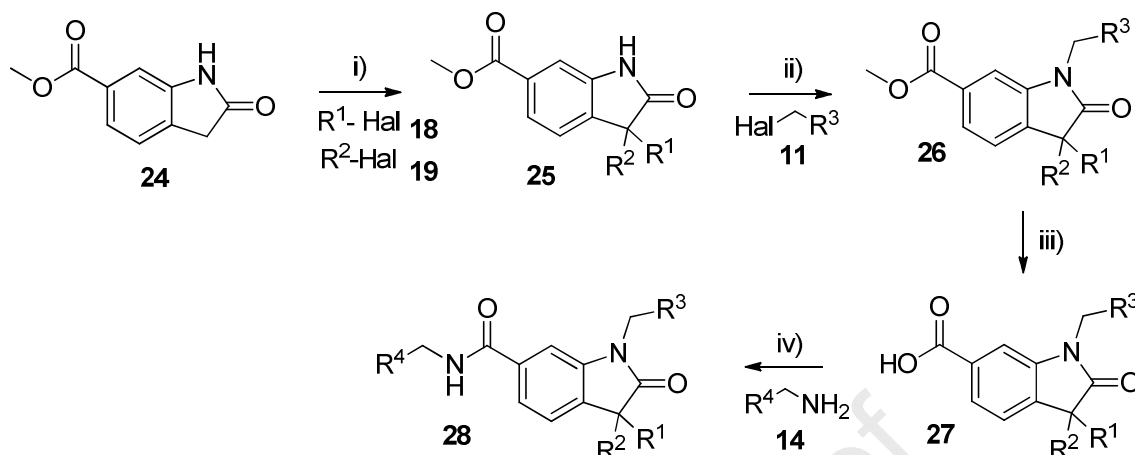
The tetrahydroquinolinone cores (**Scheme 2**) were made starting from a commercially available dihydroquinolin-2(1*H*)-one core **16**. Following a standard base-mediated *N*-alkylation to give the substituted quinolinones **17**, the core was alkylated either with a single substituent **18**

(to give **20**) or sequentially with two different substituents **18** and **19** (to give **21**) using strong base and a suitable alkyl halide. Ester hydrolysis to the corresponding acid **22** and amide coupling with a suitable amine **14** gave the final test compounds **23**.



Scheme 2. Synthesis of tetrahydroquinolinones. Reagents and conditions: i) 1,2-dichloroethane, NaOH, water, tetrabutylammonium bromide, room temperature, 68-89%; ii) LiHMDS, THF, -78°C, 17-48%; iii) MeOH, water, THF, LiOH.H₂O, room temperature, 55-94%; iv) DCM, HATU, triethylamine, room temperature, 53-67%.

Other ring sizes, such as the oxindole core, were accessed using similar methods starting from an oxindole core, as depicted in **Scheme 3**. Alkylation of 2-oxindoline-6-carboxylate ester **24** gave the alkylated core **25**. Insertion of the *N*-indoline substituent with a base-mediated alkylation reaction gave the corresponding *N*-alkyl analogues **26**. Ester hydrolysis **27** and amide formation with amines **14** as before then gave the final test compounds **28**.



Scheme 3. Example synthesis of an oxindole core. Reagents and conditions: i) DMF, NaH, -10°C, 74-79%; ii) DMF, NaH, room temperature, 52-99%; iii) MeOH, water, THF, LiOH.H₂O, room temperature, 57-99%; iv) DCM, HATU, triethylamine, room temperature, 48-85%.

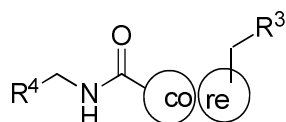
2.2 Biological testing

Compounds were evaluated in a stable HEK293T STING-expressing luciferase reporter cell line and a primary screen based on IRF3 reporter activation. Structural changes were assessed for potency in the HEK293T-hSTING-luciferase assay, tested initially at a single concentration with the most promising compounds then tested in a dose-response assay. Functional studies to confirm compound-induced STING phosphorylation used immunoblotting and cell-based activation was confirmed through multiplexed cytokine measurement. The analogues explored in this campaign used either the simple benzyl substituent of **4** or similar di-halo benzyl substituents as found in **5**, with either a 2-furanylmethyl or 2,4,6-trifluorobenzyl amide substituent.

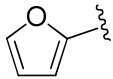
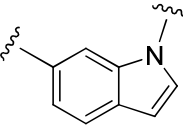
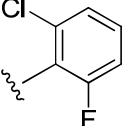
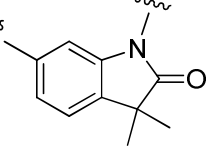
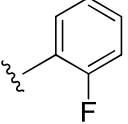
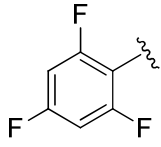
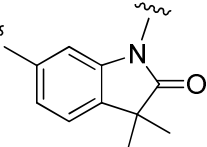
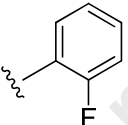
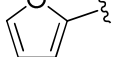
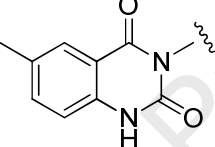
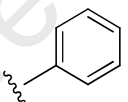
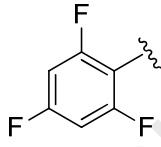
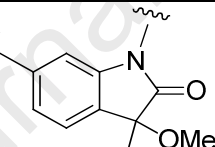
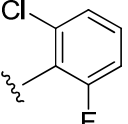
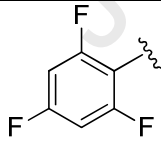
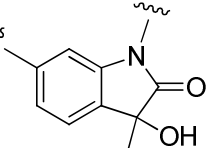
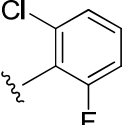
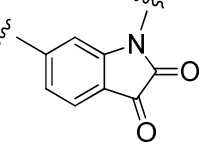
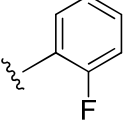
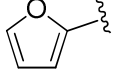
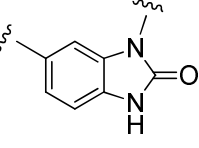
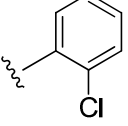
2.3 STING activity of core variations

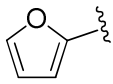
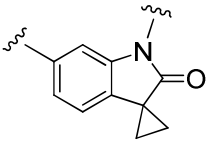
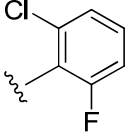
We initially investigated multiple changes to the core benzothiazinone scaffold, using either the furan or the trifluorobenzyl group as preferred amide substituents (**Table 1**).

Table 1. Core template analogues of compound **5**



Entry	R ⁴	Core variant	R ³	% activation ^s	cLogP
5				27% @ 10μM	2.7
29				30% @ 10μM	3.0
30				7% @ 100μM	2.3
31				105% @ 10μM	3.7
32				-1% @ 10μM	2.4
33				-1% @ 10μM	3.1

Entry	R ⁴	Core variant	R ³	% activation [§]	cLogP
34				-1% @ 10μM	3.9
35				73% @ 10μM	3.8
36				116% @ 1μM	5.3
37				0% @ 10μM	3.7
38- <i>rac</i>				20% @ 1μM	4.9
39- <i>rac</i>				67% @ 20μM	4.3
40				0% @ 50μM	2.5
41				-1% @ 10μM	3.4

Entry	R ⁴	Core variant	R ³	% activation [§]	cLogP
42				6% @ 10μM	3.9

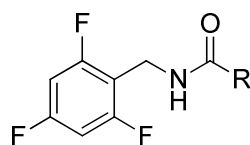
[§]Percentage activation relative to the level of activation provided by a positive control. Activation levels were measured at the stated concentration of compound.

Replacing the thio group with an oxo (**29**) equivalent was tolerated whilst the carbon version (**31**) appeared significantly more active than the benzothiazine core. The oxidised sulfoxide core **30** and the expanded oxepine core **32** were, by contrast, inactive. The quinazoline-dione **37** in which the benzyl substituent was located along a different vector relative to the position of the amide group was also inactive. We made several indole derivatives, for example the 1-indole **34** and the 3-substituted oxindole **33** which were both inactive. However, the 1-substituted oxindole **35** showed appreciable activity, and when the furan amide group was replaced with trifluorophenyl, compound **36** gained a significant boost in potency, albeit with an increase in lipophilicity. To ameliorate this increase in logP, we replaced one of the gem-dimethyl groups with a more polar isostere of Me, for example the OMe **38** and the OH **39**. These analogues became progressively less active, indicating that this region of the pharmacophore required lipophilicity for high potency. We therefore synthesized several more analogues with various substituents at the 3-position of the oxindole core. The oxo compound **40** and the benzimidazolone **41** which featured polar groups at this position were also inactive. However, when the lipophilic spiro-cyclopropane **42** was also made, it too was found to be inactive, confirming a very specific tolerance of substituents in this location.

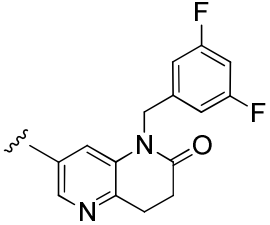
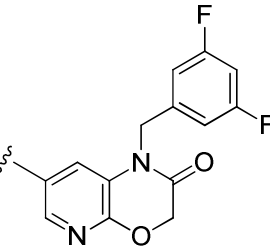
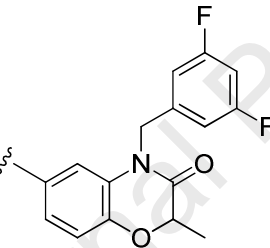
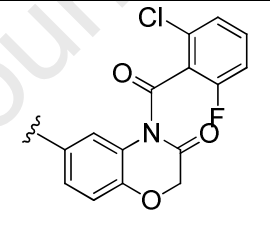
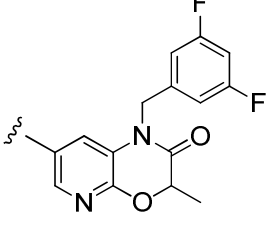
We were aware that in our previous investigations, a dihalo-benzyl substitution pattern at the R³ position and a trifluorobenzyl amide group at R⁴ were favoured and we incorporated these

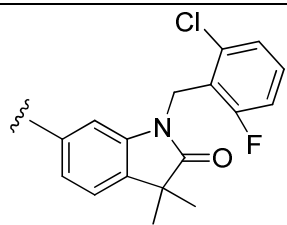
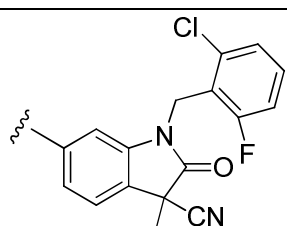
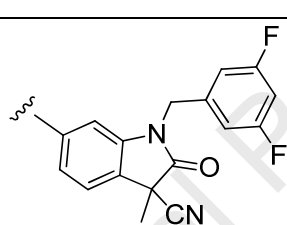
combined structural features into the more promising core changes from the compounds in **Table 1**. These structures are shown in **Table 2**. In the promising tetrahydroquinolinone series, the trifluorobenzyl amide **43** was significantly more potent than the furan equivalent. Core methylation as in **44** and **46** was tolerated but did not increase activity, while lactam isosteres such as the thiolactam derivative **45** was less potent. We also found that aza substitution in the benzene ring of the core was detrimental to activity, for example **47** and **48**. In the benzoxazine series, the trifluorobenzyl amide insertion had little effect on potency, with the aza version **49** of similar or weaker potency than the original analogue **29**. An exocyclic carbonyl linker in **51** was not tolerated, consistent with our previous observations that methylene linkers tended to be more potent. Core methylation however, provided a substantial boost in potency with the racemic methylated derivative **50** now showing similar activity to the quinolinone series of compounds, while aza substitution in this core (e.g. **52**) also led to a sharp drop in compound activity. It should be noted that attempts to resolve the chiral center in **50** by individual enantiomer synthesis were thwarted by facile racemization of this position. We were concerned that separated enantiomers of the final product would also be vulnerable to racemization which led us to put this series on hold. A description of this work is provided in the Supplementary Material. Finally, in the oxindole series, optimal substitution of the core provided highly potent STING activators e.g. **53** which had a measured EC₅₀ of 185 nM. We found that modest reductions in logP could be achieved by replacing the *gem*-dimethyl substituent with a Me or CN variation, with compounds **54** and **55** showing similar levels of potency, for example **55** had a measured EC₅₀ of 175 nM.

Table 2. Core variations with optimized R³ and R⁴ groupings



Entry	R	% activation ^s (EC ₅₀)	cLogP
43		107% @ 1μM	5.2
44- <i>rac</i>		92% @ 1μM	5.8
45- <i>rac</i>		40% @ 1μM	4.3
46		102% @ 1μM	5.6
47		5% @ 1μM	4.6

Entry	R	% activation [§] (EC ₅₀)	cLogP
48		58% @ 10μM	3.8
49		3% @ 1μM	3.4
50 <i>rac</i>		95% @ 1μM	4.5
51		26% @ 10μM	4.6
52 <i>rac</i>		6% @ 1μM	3.9

Entry	R	% activation [§] (EC ₅₀)	cLogP
53		(EC ₅₀ 185 nM)	5.7
54- <i>rac</i>		102% @ 1μM	5.6
55- <i>rac</i>		(EC ₅₀ 175 nM)	5.2

[§]Percentage activation relative to the level of activation provided by a positive control. Activation levels were measured at the stated concentration of compound.

Through this short SAR exercise, we had identified excellent sub-micromolar activity in several different core structures. We were aware that small molecule ligands in the literature were typically reported to have activity at just one or two species, and in some cases activity at a limited number of STING polymorphs. Notably, early examples of benzothiazinones did not significantly activate the HAQ haplotype [27]. Compounds from within these new core chemotypes were therefore screened for species and STING mutant activity.

2.4 Human isoform activity

A selection of compounds from the above tables were screened against three of the most common STING polymorphs, R232, H232 and HAQ (**Table 3**). All compounds tested showed excellent pan-polymorph activity across the panel of STING proteins tested against.

Table 3. Activity of selected compounds against STING polymorphs

Compound	R232.HEK293T	H232.HEK293T	HAQ.HEK293T
	% act @ 10 μ M [§]	% act @ 10 μ M [§]	% act @ 10 μ M [§]
53	92	107	92
43	102	121	86
44	116	132	99
46	114	137	107
55	122	110	98
45	120	128	93
54	113	117	92

[§]percentage activation following a challenge with a positive control in a STING expressing HEK293T cell line at a fixed concentration of each test compound

An example from **Table 3**, compound **53** was then tested in a dose response assay against all 5 of the major human STING polymorphs (**Figure 3**). **53** activated the luciferase coupled ISRE.ISG54 reporter system in R232, H232, HAQ, AQ and Q variants of human STING to varying degrees in stably transfected HEK293T cells, confirming activity across the range of polymorphs.

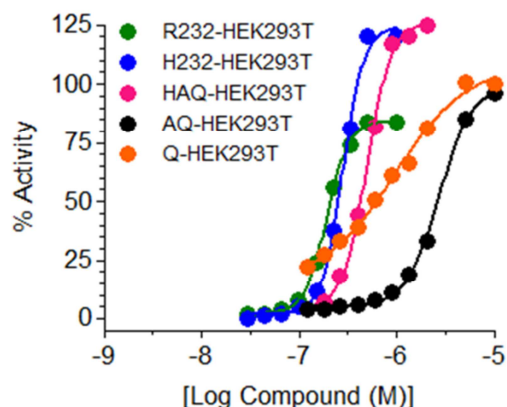


Figure 3. Compound **53** activity is STING variant dependent. **53** activates the luciferase coupled ISRE.ISG54 reporter system in the most common variants of human STING. Cells were incubated with G10 for 18 hours and luciferase activity was estimated.

2.5 STING orthologue activity

We were cognisant of the species differences at mouse and human STING proteins of DMXAA and in other series [18d] and that human STING has distinct sequence variations in the human population. Human and mouse STING are 68% identical and have 81% similarity, whilst human and rat are 69% identical and human and cynomolgus monkey more than 90% identical [28]. Consistent with our previous findings, **53** was not active at mouse STING, but was similarly potent at both human and cynomolgus monkey (data not shown).

2.6 Compound **53** is a direct STING activator

We also showed that **53** is a direct activator of STING. This was carried out biochemically, using a three component assay containing just recombinant STING, TBK1 and test compound,

assaying for phosphorylated STING protein by immunoblotting (**Figure 4**). These data demonstrated that compound **53** was a potent STING agonist in a cell free pSTING assay.

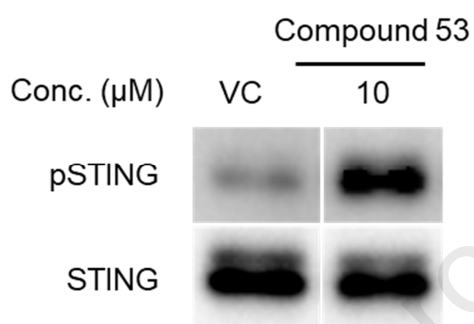


Figure 4. Compound **53** is a direct and potent STING agonist in a cell-free pSTING assay [27]. Immunoblots showing **53**-dependent phosphorylation of recombinant CTT domain of R232 STING by recombinant TBK1 enzyme (Lane 1: Vehicle control only, Lane 2: **53** at 10 μM)

2.7 Human STING variants are phosphorylated on treatment with a novel STING agonist

We further showed that **53** was able to phosphorylate various STING polymorphs in overexpressed HEK293T cells by immunoblotting (**Figure 5**). Both phosphorylated IRF3 and phosphorylated STING were produced in a dose-dependent manner when exposed to compound.

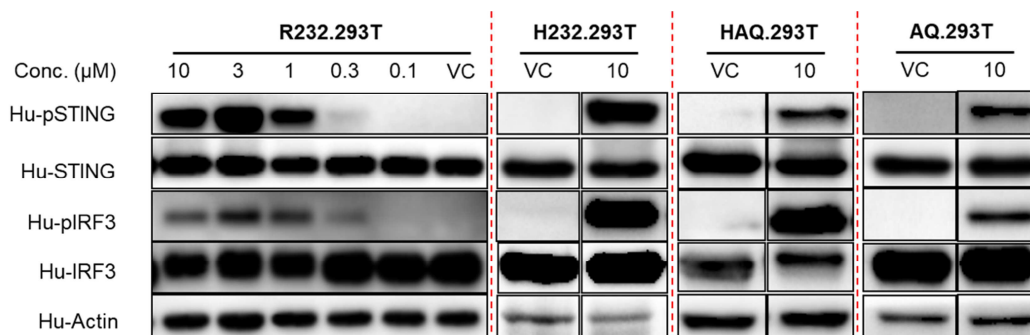
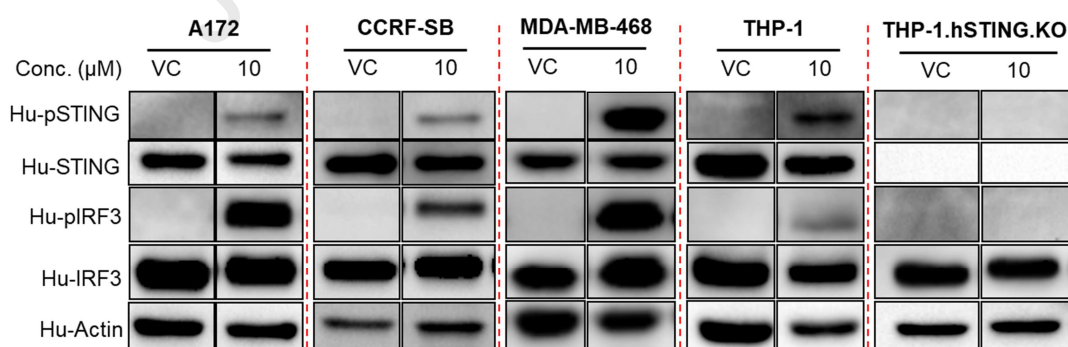


Figure 5. Compound **53** treatment leads to phosphorylation of variants of human STING in overexpressed HEK293T cells. Cells were incubated with **53** for 2 hours and then proteins harvested and analyzed by immunoblotting using human pSTING, STING, pIRF3, IRF3 and actin antibodies.

We then showed that **53** enabled phosphorylation of endogenous variants of the STING protein in various tumor cells (**Figure 6**) at a single concentration. Compound **53** led to STING and IRF3 phosphorylation across the panel of STING variants tested, except in the STING KO cells where STING was absent.



Tumor Cells	71aa	230aa	232aa	293aa	SNP type	Allelic nature
A172	R	G	R	R	R232 (WT)	Homozygous
CCRF-SB	R	G	R	R	R232 (WT)	Homozygous
THP-1	H	A	R	Q	HAQ	Homozygous
MDA-MB-468	R	G	R	R	R232 (WT)	Homozygous

Figure 6. Compound **53** treatment leads to phosphorylation of the endogenously expressed human STING variants in various tumor cells. Cells were incubated with 10 μ M **53** for 2 h and then proteins harvested and analyzed by immunoblotting using human pSTING, STING, pIRF3, IRF3 and actin antibodies with the blots shown in the first panel. The second panel shows the specific SNP pattern contained in each tumor cell line.

2.8 Treatment with a novel STING agonist leads to phosphorylation of human primary cells carrying various STING polymorphs

We next showed that **53** enabled phosphorylation of STING in human primary cells from three different donors at a single concentration (**Figure 7**).

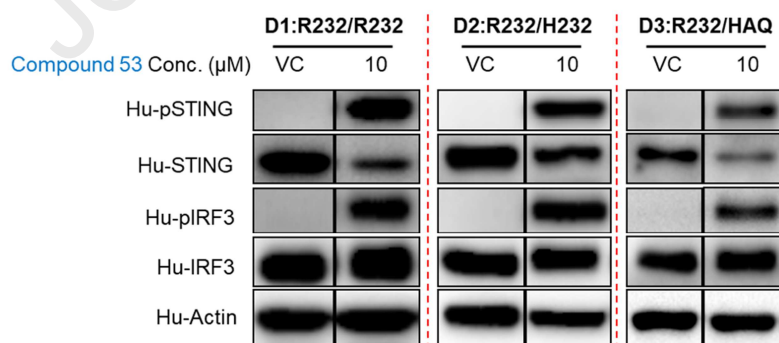


Figure 7. Compound **53** treatment leads to phosphorylation of the STING variants of human STING from three different human donors (D1, D2 & D3) PBMCs. Cells were incubated with

10 μ M **53** for 2 h and then proteins harvested and analyzed by immunoblotting using human pSTING, STING, pIRF3, IRF3 and actin antibodies.

2.9 Cytokine induction following STING activation

Human primary cells from donors were stimulated with a single concentration of **53** and levels of cytokines induced measured at an early (5h) and a late (20h) time point post-treatment (**Figure 8**).

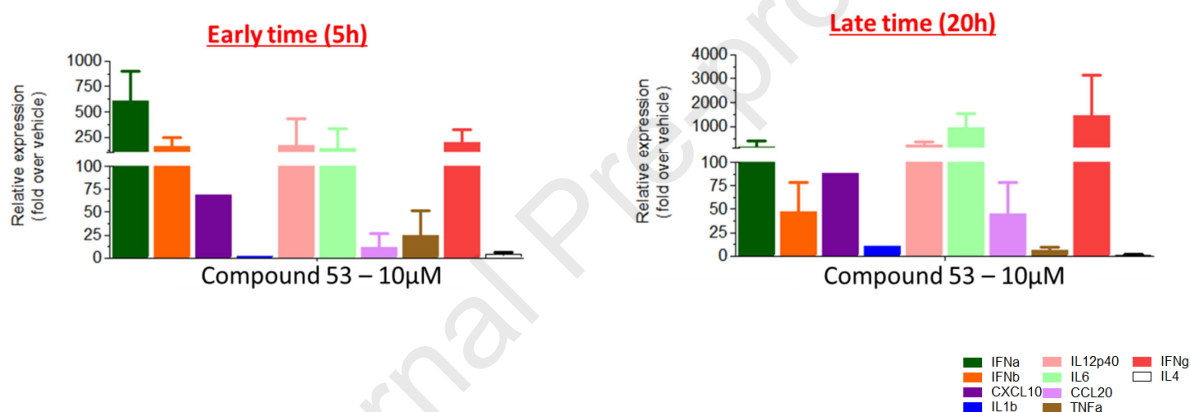


Figure 8. Compound **53** cytokine induction profile in hPBMC

A panel of ten pro-inflammatory cytokines were measured which included IFN α , IFN β , TNF α , IL6, CCL20, IL1 β , IL12p40, CXCL10, IFN γ , IL4 as indicators of activation of both the IRF3 and the NF κ B pathways. The induction of these cytokines was measured by qPCR and relative normalized expression (fold induction) was determined by comparison with vehicle treated controls. **53** at 10 μ M strongly induced the expression of most of the cytokines especially Type I IFN subtypes such as IFN β and CXCL10 which is consistent with an activated STING signature operating through the IRF3 pathway. Cytokine induction was sustained over a period

of 24 hours. It is notable that IL6, CCL20 and TNF α were also induced, indicating activation of the NF κ B pathway.

2.10 Cytokine induction and dendritic cell maturation following STING activation

Human PBMCs were isolated and treated with IL4 and GMCSF to induce hMO-DC (human monocyte derived dendritic cells). Cells from a donor harboring the R232 polymorph were stimulated with 10 μ M **53** for 20 h and several pro-inflammatory cytokines and activation markers were monitored as depicted in **Figure 9**. Six activation cytokines were selected as the more prominent markers of immune system stimulation.

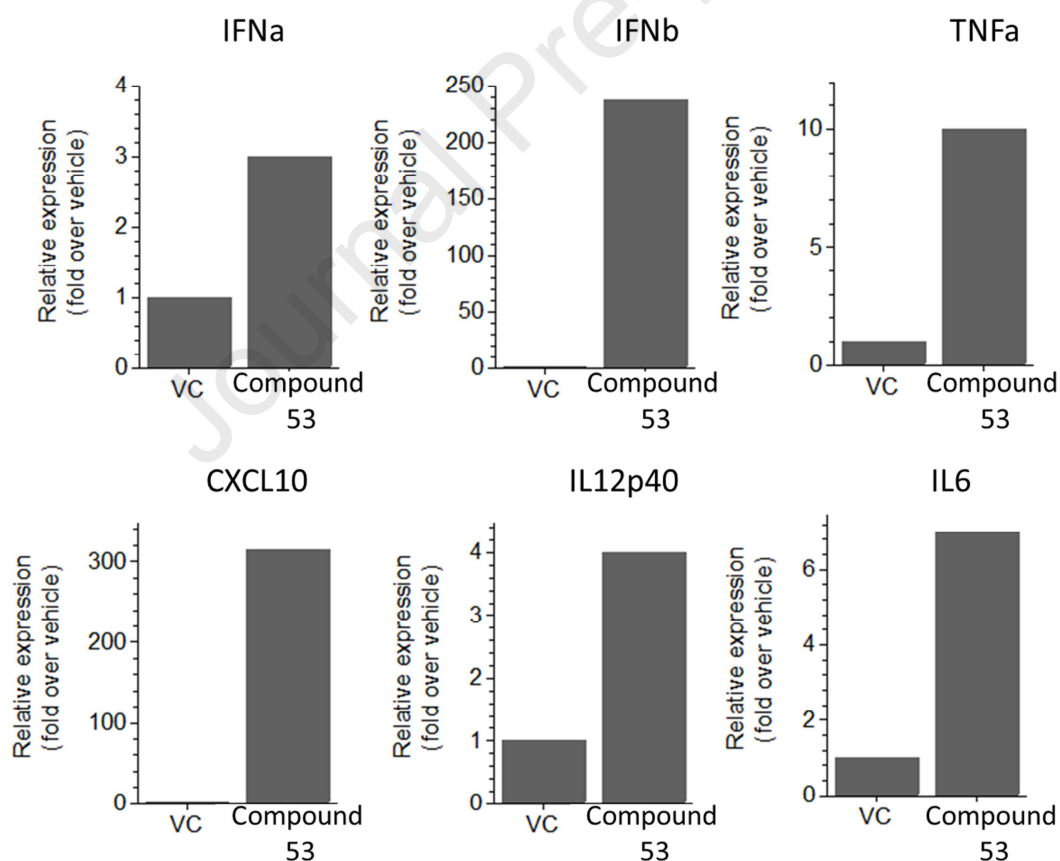


Figure 9. Cytokine induction in hMO-DCs following treatment with **53**

To productively present any antigen to T cells, DCs first have to be activated and markers can be used to indicate DC activation. CD86 and CD83 are two markers of DC activation that showed increased expression following treatment with **53** (**Figure 10**).

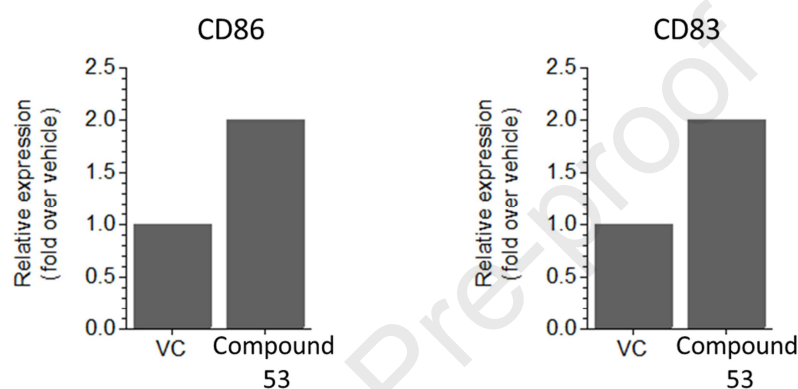


Figure 10. Dendritic cell maturation marker expression after treatment with **53**. The fold induction of the activation markers were measured by qPCR and relative normalized expression was determined by comparison with vehicle treated control

The above data showed conclusively that **53** was able to directly activate STING from across the major protein variants found in the human population and from both recombinant and primary cells. It was able to induce a broad panel of cytokines and markers of dendritic cell maturation consistent with its activation of STING.

2.11 ADMET

In order to assess the *in vivo* pharmacokinetics of **53**, we chose a rodent pharmacokinetic model to evaluate ADME properties. When dosed in mice, **53** was well-absorbed with a short terminal half-life (**Table 4** and **Figure 11**).

Table 4. Mouse pharmacokinetic profile of **53**. Compound was dosed in solution using 40% PEG, 20% PG & 10% DMA in NS.

Route	Dose (mpk)	AUC (ng/mL*h)	T _{1/2} (h)	C _{max} (ng/mL)	V _d (mL/kg)	F (%)
IV	5	1215	1.41	1867	2689	NA
PO	10	2090	NA	1723	NA	86

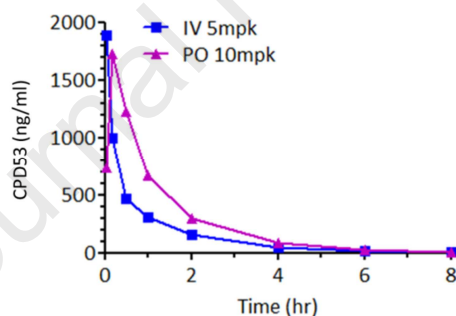


Figure 11. Pharmacokinetic profile of **53** in mouse

At 10 μ M concentration, **53** was stable in buffers across the pH range 3-8 and was stable in mouse and human plasma at 37°C demonstrating excellent chemical stability. The compound showed low CYP inhibition (**Figure 12**), did not cause any non-specific anti-proliferation in a cell-based cytotoxicity assay and possessed a large window over hERG binding (~20% inhibition at 10 μ M).

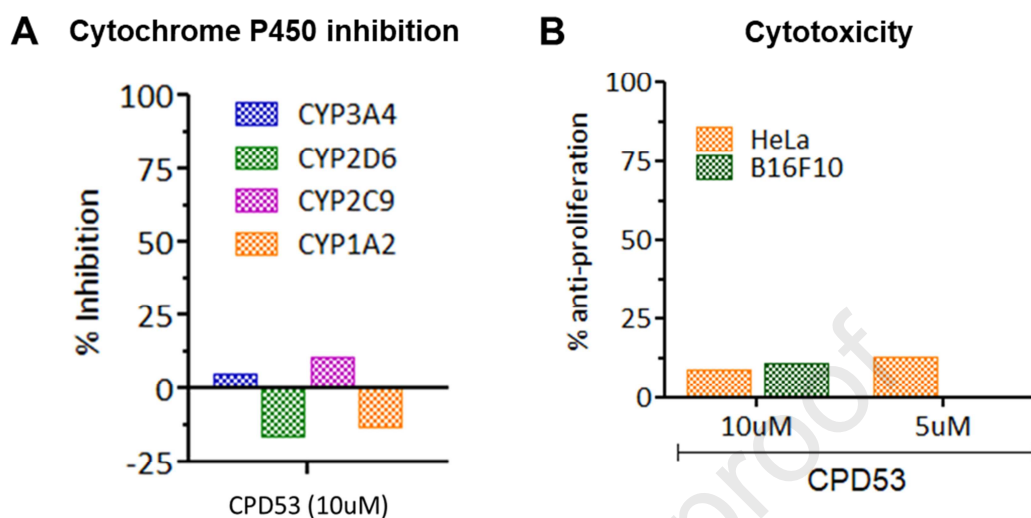


Figure 12. Cytochrome P450 inhibition (panel **A**) and cytotoxicity assessment (panel **B**) of **53**.

The compound had a low liver microsomal half-life (HLM $t_{1/2}$ ~ 10 min.), with high human plasma binding of >99.5%. This stability, absorption, selectivity and overall pharmacokinetic profile made the compound a suitable tool for further evaluation of the STING mechanism.

3 Conclusion

In summary, we have developed several novel core chemotypes as potent small molecule human STING activators with excellent functional properties in a battery of human and preclinical species testing. An example compound, **53**, activated all five major STING polymorphs and showed the expected STING phosphorylation, cytokine induction and dendritic cell maturation profile consistent with this mechanism. Further studies with compounds from these series will be reported in due course.

4 Experimental

4.1 General methods for compound synthesis

Compounds were made according to the methods described in WO2018234807, WO2018234805 and WO2018234808 and are described in detail below and in the Supporting Material. All chemicals, reagents and solvents were purchased from commercial sources and used without further purification. All reactions were performed under an atmosphere of nitrogen unless otherwise noted. Nuclear magnetic resonance (NMR) spectra were in all cases consistent with the proposed structures. Characteristic chemical shifts (δ) are given in parts-per-million downfield from tetramethylsilane using conventional abbreviations for designation of major peaks: e.g. s, singlet; d, doublet; t, triplet; q, quartet; m, multiplet; br, broad. Spectra were recorded in deuterodimethylsulphoxide; d_6 -DMSO. Mass spectra, MS (m/z), were recorded using electrospray ionisation (ESI). Where relevant and unless otherwise stated the m/z data provided are for isotopes ^{19}F , ^{35}Cl , ^{79}Br and ^{127}I . Thin layer chromatography (TLC) was carried out on Merck silica gel 60 plates (5729). All final compounds were >95% pure as judged by the LCMS or UPLC analysis methods described in the General Purification and Analytical Methods below unless otherwise stated. Flash column chromatography was carried out using pre-packed silica gel cartridges in a Combi-Flash platform. Prep-HPLC purification was carried out according to the General Purification and Analytical Methods described in the Supplementary Material.

4.2 General procedures for synthesis of benzothiazinone and benzoxazinone intermediates

4.2.1 Methyl 4-((2-ethoxy-2-oxoethyl)thio)-3-nitrobenzoate

Methyl 4-fluoro-3-nitrobenzoate (10.0 g, 50.2 mmol) was taken up in MeCN (2.0 L) and TEA (7.61 g, 75.38 mmol) was added to it. The reaction mixture was cooled to 0-5 °C and ethyl thioglycolate (7.25 g, 62.7 mmol) was added dropwise. The reaction mixture was stirred for 30 min. at ice cold temperature. Progress of the reaction was monitored by TLC and after

completion; the reaction mixture was diluted with EtOAc and washed with saturated solution of NH_4Cl and brine. The organic layer was dried over anhydrous Na_2SO_4 and evaporated under reduced pressure to dryness to give the title compound (14.0 g, 93% yield) as a yellow solid which was pure enough to be used in the next step without any further purification. LCMS m/z: 300.06 $[\text{M}+\text{H}]^+$.

4.2.2 Methyl 3-oxo-3,4-dihydro-2H-benzo[b-1,4]thiazine-6-carboxylate

To a stirred solution of methyl 4-((2-ethoxy-2-oxoethyl)thio)-3-nitrobenzoate (5.0 g, 16.7 mmol) in acetic acid (50 mL) was added iron powder (3.73 g, 66.8 mmol). The resulting reaction mixture was stirred at 80 °C for 3 h. On completion (monitored by TLC), it was cooled to room temperature and poured onto 1N HCl (250 mL) and then stirred for 1 h. The white precipitate was filtered off and washed with water. The obtained solid was re-dissolved in 5% MeOH in DCM (50 mL) and filtered through a bed of celite. The filtrate was evaporated to dryness to afford the title compound (3.5 g, 91% yield) as a golden white solid. LCMS m/z: 222.05 $[\text{M}-\text{H}]^+$.

4.2.3 Methyl 4-benzyl-3-oxo-3,4-dihydro-2H-benzo[b][1,4]thiazine-6-carboxylate

To a stirred solution of methyl 3-oxo-3,4-dihydro-2H-benzo[b-1,4]thiazine-6-carboxylate (4.0 g, 17.91 mmol) in EDC (60 mL) was added NaOH solution (1.432 g, 35.82 mmol in 60 mL H_2O) portionwise followed by TBAB (576 mg, 1.791 mmol) at RT. The whole was stirred for 30 min at RT and then benzyl bromide (3.675 g, 21.49 mmol) was added dropwise. The reaction mixture was then stirred at room temperature for 2 h. The progress of the reaction was monitored by TLC and after completion the reaction mixture was diluted with DCM, washed with water and then brine solution. The organic layer was dried over anhydrous Na_2SO_4 and evaporated under

reduced pressure to dryness to give the title compound (4.98 g, 89% yield) as crude which was used directly in the next step. LCMS m/z: 314 [M+H]⁺.

4.2.4 4-Benzyl-3-oxo-3,4-dihydro-2H-benzo[b][1,4]thiazine-6-carboxylic acid

To a stirred solution of methyl 4-benzyl-3-oxo-3,4-dihydro-2H-benzo[b][1,4]thiazine-6-carboxylate (4.98 g, 15.91 mmol) in a mixture of MeOH, water and THF (1:1:2; 40 mL) was added LiOH.H₂O (1.33 g, 31.82 mmol) at RT. The reaction was allowed to stir at RT for 2 h. Upon completion of the reaction, the solvents were evaporated under reduced pressure and the residue was dissolved in water, washed with EtOAc and then acidified to ~pH 5. The acidified aqueous solution was then extracted with EtOAc. The combined organic extracts were washed with brine, dried over anhydrous Na₂SO₄ and evaporated to dryness to give the title compound (3.2 g, 67% yield) as a white solid which was used in the next step without any further purification. LCMS m/z: 300 [M-H]⁺.

4.3 Synthesis of benzoxazinones and benzothiazinones

4.3.1 4-Benzyl-N-(furan-2-ylmethyl)-3-oxo-3,4-dihydro-2H-benzo[b][1,4]thiazine-6-carboxamide (5)

To a stirred solution of 4-benzyl-3-oxo-3,4-dihydro-2H-benzo[b][1,4]thiazine-6-carboxylic acid (120 mg, 0.401 mmol) in DMF (5 mL) was added HATU (183 mg, 0.481 mmol) followed by TEA (0.101 g, 1.0 mmol) at RT. The resulting reaction mixture was stirred at RT for 30 min. then 1-(furan-2-yl)-methanamine (38.4 mg, 0.401 mmol) was added and stirring continued at RT for 2 h. Progress of the reaction was monitored by TLC and LCMS and after completion, the reaction mixture was diluted with EtOAc and washed with chilled water and brine. The organic

layer was dried over anhydrous Na_2SO_4 and evaporated under reduced pressure to dryness. The crude material obtained was purified by prep-HPLC to afford the title compound **5** (30 mg, 19.9% yield) as a white solid. Purity UPLC: 99.29%; $^1\text{H-NMR}$ (500 MHz; DMSO-d_6): δ 3.72 (s, 2H), 4.42 (d, $J = 5.5$ Hz, 2H), 5.28 (s, 2H), 6.22 (d, $J = 2.8$ Hz, 1H), 6.39 (s, 1H), 7.20-7.24 (m, 3H), 7.29-7.32 (m, 2H), 7.51-7.54 (m, 2H), 7.57 (s, 1H), 7.65 (s, 1H), 8.99 (t, $J = 5.45$ Hz, 1H); LCMS m/z : 379.18 $[\text{M}+\text{H}]^+$; HRMS (ESI) m/z : $[\text{M}+\text{H}]^+$ calcd for $\text{C}_{21}\text{H}_{18}\text{N}_2\text{O}_3\text{S}$ 379.1116, found 379.1105.

4.3.2 4-(2-Chloro-6-fluorobenzyl)-*N*-(furan-2-ylmethyl)-3-oxo-3,4-dihydro-2*H*-benzo[*b*-1,4]oxazine-6-carboxamide (**29**)

Purity UPLC: 99.78%; $^1\text{H-NMR}$ (500 MHz; DMSO-d_6): δ 4.43 (d, $J = 5.6$ Hz, 2H), 4.75 (s, 2H), 5.33 (s, 2H), 6.24 (d, $J = 2.9$ Hz, 1H), 6.40-6.41 (m, 1H), 7.07 (d, $J = 8.35$ Hz, 1H), 7.17 (t, $J = 9.8$ Hz, 1H), 7.31-7.35 (m, 2H), 7.52-7.54 (dd, $J_1 = 1.65$ Hz, $J_2 = 8.35$ Hz, 1H), 7.58 (s, 1H), 7.68 (d, $J = 1.5$ Hz, 1H), 8.85 (t, $J = 5.6$ Hz, 1H); LCMS m/z : 414.99 $[\text{M}+\text{H}]^+$; HRMS (ESI) m/z : $[\text{M}+\text{H}]^+$ calcd for $\text{C}_{21}\text{H}_{16}\text{ClFN}_2\text{O}_4$ 415.0861, found 415.0849.

4.3.3 1-(3,5-Difluorobenzyl)-2-oxo-*N*-(2,4,6-trifluorobenzyl)-2,3-dihydro-1*H*-pyrido[2,3-*b*][1,4]oxazine-7-carboxamide (**49**)

Purity UPLC: 99.15%; $^1\text{H-NMR}$ (500 MHz; DMSO-d_6): δ 4.42 (d, $J = 4.7$ Hz, 2H), 5.10 (s, 2H), 5.17 (s, 2H), 7.09-7.19 (m, 5H), 7.57 (s, 1H), 8.32 (s, 1H), 8.98 (s, 1H); LCMS m/z : 464.24 $[\text{M}+\text{H}]^+$; HRMS (ESI) m/z : $[\text{M}+\text{H}]^+$ calcd for $\text{C}_{22}\text{H}_{14}\text{F}_5\text{N}_3\text{O}_3$ 464.1034, found 464.1021.

4.3.4 2-Methyl-4-(3,5-difluorobenzyl)-3-oxo-N-(2,4,6-trifluorobenzyl)-3,4-dihydro-2H-1,4-benzoxazine-6-carboxamide (**50**)

Purity UPLC: 99.59%; ¹H-NMR (500 MHz; DMSO-d₆): δ 1.53 (d, *J* = 6.65 Hz, 3H), 4.41 (s, 2H), 5.02-5.10 (m, 2H), 5.29 (d, *J* = 16.8 Hz, 1H), 6.99 (d, *J* = 6.5 Hz, 2H), 7.11-7.17 (m, 4H), 7.41 (s, 1H), 7.53 (d, *J* = 8.25 Hz, 1H), 8.73 (bs, 1H); LCMS m/z: 477.28 [M+H]⁺; HRMS (ESI) m/z: [M+H]⁺ calcd for C₂₄H₁₇F₅N₂O₃ 477.1238, found 477.1235.

4.3.5 1-(3,5-Difluorobenzyl)-3-methyl-2-oxo-N-(2,4,6-trifluorobenzyl)-2,3-dihydro-1H-pyrido[2,3-b][1,4]oxazine-7-carboxamide (**52**)

Purity UPLC: 98.99%; ¹H-NMR (500 MHz; DMSO-d₆): δ 1.58 (d, *J* = 6.75 Hz, 3H), 4.43 (bs, 2H), 5.25-5.29 (m, 2H), 7.05 (d, *J* = 6.65 Hz, 2H), 7.17 (t, *J* = 8.65 Hz, 3H), 7.64 (s, 1H), 8.35 (s, 1H), 8.89 (bs, 1H); LCMS m/z: 478.30 [M+H]⁺; HRMS (ESI) m/z: [M+H]⁺ calcd for C₂₃H₁₆F₅N₃O₃ 478.1190, found 478.1177.

4.3.6 4-(2-Chloro-6-fluorobenzoyl)-N-(2,4,6-trifluorobenzyl)-3,4-dihydro-2H-benzo[b][1,4]oxazine-6-carboxamide (**51**)

Purity UPLC: 98.96%; ¹H-NMR (500 MHz; DMSO-d₆): δ 3.68 (bs, 1H), 3.94-3.98 (m, 0.5H), 4.32 (bs, 2H), 4.45 (s, 2H), 6.94-7.03 (m, 2H), 7.20-7.29 (m, 3H), 7.45-7.53 (m, 2H), 7.60-7.66 (m, 1H), 8.54-8.58 (m, 0.5H), 8.75-8.86 (m, 1H); LCMS m/z: 479.23 [M+H]⁺; HRMS (ESI) m/z: [M+H]⁺ calcd for C₂₃H₁₅ClF₄N₂O₃ 479.0786, found 479.0783.

4.3.7 4-(2-Chloro-6-fluorobenzyl)-N-(furan-2-ylmethyl)-3-oxo-3,4-dihydro-2H-benzo[b][1,4]thiazine-6-carboxamide 1-oxide (**30**)

Purity UPLC: 99.62%; $^1\text{H-NMR}$ (500 MHz; DMSO-d_6): δ 4.28 (s, 2H), 4.48 (t, $J = 4.75$ Hz, 2H), 5.36 (d, $J = 15.9$ Hz, 1H), 5.45 (d, $J = 15.9$ Hz, 1H), 6.29 (d, $J = 2.8$ Hz, 1H), 6.41-6.42 (m, 1H), 7.15 (t, $J = 9.05$ Hz, 1H), 7.30-7.35 (m, 2H), 7.60 (d, $J = 0.8$ Hz, 1H), 7.73 (d, $J = 7.9$ Hz, 1H), 7.92 (d, $J = 8.1$ Hz, 2H), 9.18 (t, $J = 5.5$ Hz, 1H); LCMS m/z: LCMS m/z: 447.09 $[\text{M}+\text{H}]^+$; HRMS (ESI) m/z: $[\text{M}+\text{H}]^+$ calcd for $\text{C}_{21}\text{H}_{16}\text{ClFN}_2\text{O}_4$ 447.0582, found 447.0570.

4.4 General procedures for synthesis of tetrahydroquinolinone intermediates

4.4.1 Methyl-1-(2-chloro-6-fluorobenzyl)-2-oxo-1,2,3,4-tetrahydroquinoline-7-carboxylate

Methyl-1-(2-chloro-6-fluorobenzyl)-2-oxo-1,2,3,4-tetrahydroquinoline-7-carboxylate was prepared from commercially available methyl 2-oxo-1,2,3,4-tetrahydroquinoline-7-carboxylate and 2-chloro-6-fluoro-benzyl chloride using an identical method to that described for **5**. LCMS m/z: 348.14 $[\text{M}+\text{H}]^+$.

4.4.2 1-(2-Chloro-6-fluorobenzyl)-2-oxo-1,2,3,4-tetrahydroquinoline-7-carboxylic acid

To a stirred solution of methyl 1-(2-chloro-6-fluorobenzyl)-2-oxo-1,2,3,4-tetrahydroquinoline-7-carboxylate (200 mg, 0.576 mmol) in a mixture of solvents THF, H_2O and MeOH (2:1:1, 8 mL) was added $\text{LiOH}\cdot\text{H}_2\text{O}$ (48.35 mg, 1.152 mmol) at 0-5 $^\circ\text{C}$. The reaction mixture was stirred at RT overnight. After completion of the reaction (monitored by TLC and LCMS) the reaction mixture was diluted with water and washed with EtOAc. The aqueous layer was acidified with 1N HCl solution and extracted with EtOAc. The combined organics were dried over anhydrous Na_2SO_4 , filtered and concentrated under reduced pressure to afford the title compound (180 mg, 94% yield) as a white solid. LCMS m/z: 334.06 $[\text{M}+\text{H}]^+$.

4.4.3 *Methyl-1-(2-chloro-6-fluorobenzyl)-3-methyl-2-oxo-1,2,3,4-tetrahydroquinoline-7-carboxylate*

To a stirred solution of methyl 1-(2-chloro-6-fluorobenzyl)-2-oxo-1,2,3,4 tetrahydroquinoline-7-carboxylate (0.6 g, 0.28 mmol) in dry THF (20 mL) was added LiHMDS (1.6 mL, 2.07 mmol) at -78 °C and the combined mixture was allowed to stir for 15 min. at -78 °C followed by addition of MeI (0.16 mL, 2.07 mmol) and the whole maintained at -78 °C for 30 min. After completion of the reaction (monitored by TLC or and LCMS), the reaction mixture was quenched with water, extracted with EtOAc, dried and evaporated to obtain the crude product which was purified by Combi-flash (4.0 g column) and eluted with 32% EtOAc in hexanes to afford the title compound (0.11 g, 17% yield) as a colorless oil. LCMS m/z: 362.21 [M+H]⁺.

4.5 *Synthesis of tetrahydroquinolinones*

4.5.1 *1-(2-Chloro-6-fluorobenzyl)-N-(furan-2-ylmethyl)-2-oxo-1,2,3,4-tetrahydroquinoline-7-carboxamide (31)*

To a stirred solution of 1-(2-chloro-6-fluorobenzyl)-2-oxo-1,2,3,4-tetrahydroquinoline-7-carboxylic acid (50 mg, 0.150 mmol) in DCM (5 mL) was added HATU (62.78 mg, 0.165 mmol) followed by DIPEA (0.065 mL, 0.375 mmol) at RT. The resulting reaction mixture was stirred at RT for 30 min., then furan-2-ylmethanamine (17.48 mg, 0.0158 mL, 0.180 mmol) was added and stirring continued at RT for 4 h. After this, the reaction mixture was diluted with EtOAc and washed with chilled water and brine. The organic layer was dried over anhydrous Na₂SO₄ and evaporated under reduced pressure to dryness. The crude material obtained was purified by prep-HPLC to afford the title compound **31** (30 mg, 48.5% yield) as a white solid. Purity UPLC: 98.09%; ¹H-NMR (500 MHz; DMSO-d₆): δ 2.60 (t, *J* = 7.6 Hz, 2H), 2.88 (t, *J* =

6.55 Hz, 2H), 4.43 (d, $J = 5.65$ Hz, 2H), 5.31 (s, 2H), 6.24 (d, $J = 2.8$ Hz, 1H), 6.40-6.41 (m, 1H), 7.12-7.16 (m, 1H), 7.27-7.33 (m, 3H), 7.46-7.48 (m, 1H), 7.57-7.59 (m, 2H), 8.90 (t, $J = 5.5$ Hz, 1H); LCMS m/z : 413.10 $[M+H]^+$; HRMS (ESI) m/z : $[M+H]^+$ calcd for $C_{22}H_{18}ClFN_2O_3$ 413.1068, found 413.1061.

4.5.2 1-(2-Chloro-6-fluorobenzyl)-2-oxo-N-(2,4,6-trifluorobenzyl)-1,2,3,4-tetrahydroquinoline-7-carboxamide (43)

Purity UPLC: 99.09%; 1H -NMR (500 MHz; DMSO- d_6): δ 2.59 (t, $J = 7.65$ Hz, 2H), 2.86 (t, $J = 6.75$ Hz, 2H), 4.43 (d, $J = 4.95$ Hz, 2H), 5.30 (s, 2H), 7.13 (t, $J = 9.35$ Hz, 1H), 7.21 (t, $J = 8.55$ Hz, 2H), 7.26-7.33 (m, 3H), 7.41 (d, $J = 7.75$ Hz, 1H), 7.51 (s, 1H), 8.78 (t, $J = 5.15$ Hz, 1H); LCMS m/z : 477.24 $[M+H]^+$; HRMS (ESI) m/z : $[M+H]^+$ calcd for $C_{24}H_{17}ClF_4N_2O_2$ 477.0993, found 477.0981.

4.5.3 8-(3,5-Difluorobenzyl)-7-oxo-N-(2,4,6-trifluorobenzyl)-5,6,7,8-tetrahydro-1,8-naphthyridine-2-carboxamide (47)

Purity HPLC: 98.25%; 1H -NMR (400 MHz; DMSO- d_6): δ 2.76 (t, $J = 7.60$ Hz, 2H), 3.01 (t, $J = 7.08$ Hz, 2H), 4.49 (d, $J = 5.56$ Hz, 2H), 5.37 (s, 2H), 6.96-7.00 (m, 3H), 7.11 (t, $J = 8.32$ Hz, 2H), 7.63 (d, $J = 7.76$ Hz, 1H), 7.81 (d, $J = 7.28$ Hz, 1H), 8.63 (bs, 1H); LCMS m/z : 462.2 $[M+H]^+$; HRMS (ESI) m/z : $[M+H]^+$ calcd for $C_{23}H_{16}F_5N_3O_2$ 462.1241, found 462.1226.

4.5.4 5-(3,5-Difluorobenzyl)-6-oxo-N-(2,4,6-trifluorobenzyl)-5,6,7,8-tetrahydro-1,5-naphthyridine-3-carboxamide (48)

Purity HPLC: 98.16%; ^1H NMR (400 MHz; DMSO- d_6): δ 2.87 (t, $J = 7.76$ Hz, 2H), 3.18 (t, $J = 7.12$ Hz, 2H), 4.43 (d, $J = 4.24$ Hz, 2H), 5.15 (s, 2H), 6.68 (d, $J = 6.24$ Hz, 2H), 7.09-7.18 (m, 3H), 7.51 (s, 1H), 8.56 (s, 1H), 9.02 (bs, 1H); LCMS m/z : 462.1 $[\text{M}+\text{H}]^+$; HRMS (ESI) m/z : $[\text{M}+\text{H}]^+$ calcd for $\text{C}_{23}\text{H}_{16}\text{F}_5\text{N}_3\text{O}_2$ 462.1241, found 462.1227.

4.5.5 1-(2-Chloro-6-fluorobenzyl)-3-methyl-2-oxo-N-(2,4,6-trifluorobenzyl)-1,2,3,4-tetrahydroquinoline-7-carboxamide (44)

Purity UPLC: 99.12%; ^1H -NMR (500 MHz; DMSO- d_6): δ 1.14 (d, $J = 6.4$ Hz, 3H), 2.56-2.68 (m, 2H), 2.93-2.96 (m, 1H), 4.39-4.48 (m, 2H), 5.16 (d, $J = 15.85$ Hz, 1H), 5.45 (d, $J = 15.9$ Hz, 1H), 7.10-7.14 (m, 1H), 7.21 (t, $J = 8.7$ Hz, 2H), 7.27-7.32 (m, 3H), 7.41-7.43 (dd, $J_1 = 7.7$ Hz, $J_2 = 0.95$ Hz, 1H), 7.50 (s, 1H), 8.78 (t, $J = 5.1$ Hz, 1H); LCMS m/z : 491.27 $[\text{M}+\text{H}]^+$; HRMS (ESI) m/z : $[\text{M}+\text{H}]^+$ calcd for $\text{C}_{25}\text{H}_{19}\text{ClF}_4\text{N}_2\text{O}_2$ 491.1149, found 491.1141.

*4.5.6 1-(3,5-Difluorobenzyl)-3-methyl-N-(2,4,6-trifluorobenzyl)-3,4-dihydro-1H-benzo[*c*][1,2]thiazine-7-carboxamide 2,2-dioxide (45)*

Purity UPLC: 95.28%; ^1H -NMR (500 MHz; DMSO- d_6): δ 1.36 (d, $J = 4.9$ Hz, 3H), 3.20-3.15 (m, 1H), 3.54 (d, $J = 16.6$ Hz, 1H), 3.83 (bs, 1H), 4.41 (s, 2H), 5.07 (s, 2H), 7.20-7.11 (m, 6H), 7.32 (d, $J = 7.2$ Hz, 1H), 7.49 (d, $J = 6.8$ Hz, 1H), 8.84 (s, 1H); LCMS m/z : 511.1 $[\text{M}+\text{H}]^+$; HRMS (ESI) m/z : $[\text{M}+\text{H}]^+$ calcd for $\text{C}_{24}\text{H}_{19}\text{F}_5\text{N}_2\text{O}_3\text{S}$ 511.1115, found 511.1104.

4.5.7 1-(3,5-Difluorobenzyl)-4,4-dimethyl-2-oxo-N-(2,4,6-trifluorobenzyl)-1,2,3,4-tetrahydroquinoline-7-carboxamide (46)

Purity HPLC: 99.63%; $^1\text{H-NMR}$ (400 MHz; DMSO-d_6): δ 1.26 (s, 6H), 2.66 (s, 2H), 4.41 (d, $J = 4.92$ Hz, 2H), 5.20 (s, 2H), 6.93-6.94 (m, 2H), 7.10-7.16 (m, 3H), 7.32 (s, 1H), 7.43 (d, $J = 8.0$ Hz, 1H), 7.53 (d, $J = 7.84$ Hz, 1H), 8.85 (t, $J = 4.88$ Hz, 1H); LCMS m/z : 489.1 $[\text{M}+\text{H}]^+$; HRMS (ESI) m/z : $[\text{M}+\text{H}]^+$ calcd for $\text{C}_{26}\text{H}_{21}\text{F}_5\text{N}_2\text{O}_2$ 489.1601, found 489.1593.

4.6 General procedures for synthesis of benzoxazepinone intermediates

4.6.1 Methyl 3-(benzylamino)-4-hydroxybenzoate

To a stirred solution of methyl 3-amino-4-hydroxybenzoate (500 mg, 2.99 mmol) in DCM (20 mL) was added benzaldehyde (0.610 mL, 5.985 mmol) followed by AcOH (0.3 mL) and the whole was allowed to stir at RT for 5 min. before sodium triacetoxyborohydride (1.795 g, 8.47 mmol) was added. The resulting reaction mixture was stirred at RT for 12 h. Progress of the reaction was monitored by UPLC-MS and TLC, and after completion the reaction mixture was washed with water and extracted with EtOAc. The organic layer was dried over anhydrous Na_2SO_4 , concentrated *in vacuo* to give a crude product which was purified by column chromatography to afford the title compound (477 mg, 62% yield) as a light yellow solid. LCMS m/z : 258 $[\text{M}+\text{H}]^+$.

4.6.2 Methyl 5-benzyl-4-oxo-2,3,4,5-tetrahydrobenzo[b][1,4]oxazepine-7-carboxylate

To a stirred solution of methyl 3-(benzylamino)-4-hydroxybenzoate (424 mg, 1.649 mmol) in CHCl_3 (7.5 mL) and water (7.5 mL) was added NaHCO_3 (568 mg, 6.764 mmol) and TBAB (265 mg, 0.824 mmol) and whole stirred at RT for 15 min. then 3-chloropropanoyl chloride (0.236 mL, 2.474 mmol) was added and the resulting reaction mixture was stirred at RT for overnight. Progress of the reaction was monitored by UPLC-MS and TLC and after completion; the

reaction mixture was washed with water and extracted with EtOAc. The organic layer was dried over anhydrous Na_2SO_4 , and concentrated *in vacuo* to give a crude product which was purified by column chromatography to afford the title compound (180 mg, 35% yield) as an off white solid. LCMS m/z: 312 $[\text{M}+\text{H}]^+$.

4.6.3 5-Benzyl-4-oxo-2,3,4,5-tetrahydrobenzo[b][1,4]oxazepine-7-carboxylic acid

To a stirred solution of methyl 5-benzyl-4-oxo-2,3,4,5-tetrahydrobenzo[b][1,4]oxazepine-7-carboxylate (175 mg, 0.562 mmol) in a mixture of solvents THF (4.0 mL), MeOH (1 mL) and water (2 mL) was added LiOH.H₂O (70.8 mg, 1.687 mmol) at 0-5 °C and the resulting reaction mixture was stirred at RT for 12 h. TLC showed complete consumption of the ester, and then solvents were evaporated *in vacuo* to give a residue which was diluted with water and washed with diethyl ether. The aqueous layer was acidified with 1N HCl and extracted with EtOAc. The combined organics were dried over anhydrous Na_2SO_4 , concentrated *in vacuo* to give the title compound (134 mg, 80 % yield) as an off white solid. LCMS m/z: 298 $[\text{M}+\text{H}]^+$.

4.7 Synthesis of benzoxazepinones

4.7.1 5-Benzyl-N-(furan-2-ylmethyl)-4-oxo-2,3,4,5-tetrahydrobenzo[b][1,4]oxazepine-7-carboxamide (32)

To a stirred solution of 5-benzyl-4-oxo-2,3,4,5-tetrahydrobenzo[b][1,4]oxazepine-7-carboxylic acid (140 mg, 0.466 mmol) in DMF (5.0 mL) was added DIPEA (0.203 mL, 1.166 mmol) and HATU (196 mg, 0.0513 mmol). The whole was stirred at RT for 15 min., then furan-2-ylmethanamine (0.05 mL, 0.559 mmol) was added dropwise and the combined mixture allowed to stir at RT for 2 h. Progress of the reaction was monitored by UPLC and TLC and after

completion; the reaction the solvent was evaporated *in vacuo* to give a residue which was diluted with water and extracted with EtOAc. The combined organic layers were washed with water followed by brine and dried over anhydrous Na₂SO₄, and concentrated *in vacuo* to give the crude product which was purified by prep-HPLC to afford the title compound **32** (50 mg, 28% yield) as a white solid. Purity UPLC: 98.77%; ¹H-NMR (400 MHz; DMSO-d₆): δ 4.36-4.39 (m, 3H), 5.26 (d, *J* = 14.8 Hz, 1H), 5.53-5.56 (m, 1H), 5.94-6.01 (m, 1H), 6.15-6.22 (m, 2H), 6.36 (dd, *J*' = 1.84 Hz, *J*'' = 3.04 Hz, 1H), 6.84 (d, *J* = 8.08 Hz, 1H), 7.14-7.25 (m, 7H), 7.38 (d, *J* = 1.4 Hz, 1H), 7.53 (d, *J* = 0.92 Hz, 1H), 8.88 (t, *J* = 5.36 Hz, 1H); LCMS *m/z*: 377.25 [M+H]⁺; HRMS (ESI) *m/z*: [M+H]⁺ calcd for C₂₂H₂₀N₂O₄ 377.1501, found 377.1492.

4.8 General procedures for synthesis of indole intermediates

4.8.1 Methyl 3-benzyl-2-oxoindoline-5-carboxylate

To a stirred solution of commercially available methyl 2-oxoindoline-5-carboxylate (500 mg, 2.618 mmol) in EtOH (15.0 mL) was added benzaldehyde (0.293 mL, 2.877 mmol) and piperidine (0.025 mL, 0.261 mmol). The resulting reaction mixture was heated at 90 °C for 5 h. TLC and LCMS showed formation of the desired unsaturated intermediate which was diluted with EtOAc followed by the addition of Pd/C (200 mg, 10% on carbon) and stirred at RT for 1 h. TLC showed complete consumption of the unsaturated intermediate and formation of the product. The reaction mixture was filtered through celite bed and washed with EtOAc. The filtrate was concentrated *in vacuo* to afford the title compound (510 mg, 69% yield) as a faint brownish solid. LCMS *m/z*: 282 [M+H]⁺.

4.8.2 Methyl 3-benzyl-1,3-dimethyl-2-oxoindoline-5-carboxylate

To a stirred solution of methyl 3-benzyl-2-oxoindoline-5-carboxylate (200 mg, 0.711 mmol) in DMF (5.0 mL) was added Cs₂CO₃ (463 mg, 1.423 mmol) followed by MeI (0.09 mL, 1.423 mmol) and the resulting reaction was stirred at RT for 3 h. Progress of the reaction was monitored by TLC and LCMS and after completion; the reaction mixture was diluted with water and extracted with EtOAc, the organic layer was washed with brine, dried over anhydrous Na₂SO₄ and the solvent was evaporated *in vacuo* to afford the crude product which was purified by Combi-flash to afford the title compound (240 mg, 109% yield trapped with DMF) as a yellow sticky solid. LCMS m/z: 310 [M+H]⁺.

4.8.3 3-Benzyl-1,3-dimethyl-2-oxoindoline-5-carboxylic acid

A stirred solution of methyl 3-benzyl-1,3-dimethyl-2-oxoindoline-5-carboxylate (240 mg, 0.776 mmol) in a mixture of AcOH (2.5 mL) and HCl (2.5 mL) was heated at 80 °C for 3 h. Progress of the reaction was monitored by TLC and LCMS and after completion; the reaction mixture was cooled to RT and the precipitate was filtered and dried to afford the title compound (120 mg, 52% yield) as a faint yellow solid. LCMS m/z: 296 [M+H]⁺.

4.8.4 Methyl 3,3-dimethyl-2-oxoindoline-6-carboxylate

To a stirred solution of commercially available methyl 2-oxoindoline-6-carboxylate (5.0 g, 26.16 mmol) in DMF (150 mL) was added MeI (7.42 g, 52.34 mmol) and the mixture was cooled to between 0 to -10 °C followed by portionwise addition of NaH (2.19 g, 54.27 mmol, 60% suspension in mineral oil). The whole was allowed to stir at between 0 to -10 °C for 1 h. The progress of the reaction was monitored by TLC. After completion of the reaction, the mixture was diluted with water, extracted with EtOAc, and the combined organic layers were washed

with brine and dried over anhydrous Na_2SO_4 . The dried organics were evaporated under reduced pressure to obtain a crude residue which was purified by Combi-flash using 35-50% EtOAc in hexanes as eluent to afford the title compound (4.4 g, 77% yield) as a light orange solid. LCMS m/z : 220.03 $[\text{M}+\text{H}]^+$.

4.8.5 Methyl 2,3-dioxindoline-6-carboxylate

To a stirred solution of methyl 2-oxoindoline-6-carboxylate (10.0 g, 52.33 mmol) in 1,4-dioxane (500 mL) was added selenium dioxide (27.9 g, 261.68 mmol) and the resulting reaction mixture was stirred vigorously at 100 °C for 1 h. After completion of the reaction (monitored by LCMS), the reaction mixture was diluted with EtOAc and water and filtered through a bed of celite. The filtrate layers were separated and the organic layer was washed with water and brine, dried over anhydrous Na_2SO_4 and then evaporated under reduced pressure to provide the crude product. This was purified by Combi-flash using 50% EtOAc in hexanes as eluent to afford the title compound (3.5 g, 34% yield) as a light yellow solid. LCMS m/z : 206 $[\text{M}+\text{H}]^+$.

4.8.6 Methyl 1-(2-chloro-6-fluorobenzyl)-3-hydroxy-3-methyl-2-oxoindoline-6-carboxylate

To a stirred solution of methyl 1-(2-chloro-6-fluorobenzyl)-2,3-dioxindoline-6-carboxylate (0.8 g, 2.30 mmol) in dry THF (25 mL) at 0-5 °C was added a solution of MeMgBr (1.15 mL, 3.45 mmol, 3M solution in diethyl ether) and the resulting reaction mixture was stirred at 0-25 °C for 16 h. The reaction was monitored by TLC, and after completion of the reaction, the reaction mixture was quenched with aqueous 1N HCl solution and extracted with EtOAc. The organic layers were washed with brine, dried over anhydrous Na_2SO_4 and evaporated under reduced pressure to obtain the crude product which was purified by Combi-flash using 60% EtOAc in

hexane as eluent to afford the title compound (0.6 g, 71% yield) as a yellow solid. LCMS m/z: 346.18 [M-17]⁺.

4.8.7 1-(2-Chloro-6-fluorobenzyl)-3-hydroxy-3-methyl-2-oxindoline-6-carboxylic acid

A stirred solution of methyl 1-(2-chloro-6-fluorobenzyl)-3-hydroxy-3-methyl-2-oxindoline-6-carboxylate (0.4 g, 1.10 mmol) in a mixture of HCl and concentrated AcOH (1:1; 8 mL) was heated at 80 °C for 5 h. After completion, the reaction mixture was cooled to 0-5 °C. The resulting precipitate was filtered, washed with cold water and hexane, then dried under reduced pressure at 50-60 °C to afford the title compound (0.34 g of crude) as a pink solid. LCMS m/z: 350.17 [M+H]⁺ & 332.12 [M-17]⁺.

4.8.8 Methyl 1-(2-chloro-6-fluorobenzyl)-3-methoxy-3-methyl-2-oxindoline-6-carboxylate

To a stirred solution of methyl 1-(2-chloro-6-fluorobenzyl)-3-hydroxy-3-methyl-2-oxindoline-6-carboxylate (100 g, 0.275 mmol) in DMF (2 mL) was added MeI (0.02 mL, 0.33 mmol) followed by portionwise addition of NaH (15 mg, 413 mmol, 60% dispersion in mineral oil) at 0-5 °C and the resulting mixture was allowed to stir at 0-5 °C for 30 min. UPLC and TLC showed formation of the desired product. The reaction mixture was diluted with water and extracted with EtOAc, the organic layer was dried over Na₂SO₄ and evaporated to yield a crude material which was purified by Combi-flash to afford the title compound (90 mg, 86% yield) as a pale yellow solid. LCMS m/z: 378 [M+H]⁺.

4.8.9 1-(2-Chloro-6-fluorobenzyl)-3-methoxy-3-methyl-2-oxindoline-6-carboxylic acid

To a stirred solution of methyl 1-(2-chloro-6-fluorobenzyl)-3-methoxy-3-methyl-2-oxindoline-6-carboxylate (80 mg, 0.212 mmol) in a mixture of solvents THF (10 mL) and water (5 mL) was added NaOH (34 mg, 0.84 mmol) at RT and the resulting reaction mixture was stirred at RT for 16 h. Progress of the reaction was monitored by TLC and after completion the reaction mixture was concentrated to give a residue. The residue was diluted with water and washed with ether. The aqueous layer was acidified with 1N HCl to produce a precipitate. The precipitate was filtered and dried in a vacuum oven to afford the title compound (70 mg, 90% yield) as a faint yellow solid. LCMS m/z: 364 [M+H]⁺.

4.8.10 3-Chloro-1-(2-chloro-6-fluorobenzyl)-3-methyl-2-oxo-N-(2,4,6-trifluorobenzyl)indoline-6-carboxamide

To a stirred solution of 1-(2-chloro-6-fluorobenzyl)-3-hydroxy-3-methyl-2-oxo-N-(2,4,6-trifluorobenzyl)indoline-6-carboxamide **39** (1.0 g, 2.03 mmol) in DCM (100 mL) was added pyridine (0.328 mL, 4.06 mmol) and SOCl₂ (0.593 mL, 8.12 mmol) at 0-5 °C. The whole was stirred at this temperature for 30 min. TLC and LCMS showed consumption of the starting material and formation of the desired compound. After completion the reaction mixture was diluted with water and extracted with DCM, the organic layer was washed with dilute HCl, dried and evaporated to give a crude product which was purified by Combi-flash to afford the title compound (477 mg, 46.31% yield) as an off white solid. ¹H-NMR(500 MHz; DMSO-d₆): δ 1.85 (s, 3H), 4.44 (d, *J* = 4.9 Hz, 2H), 5.04 (d, *J* = 15.6 Hz, 1H), 5.14 (d, *J* = 15.6 Hz, 1H), 7.19-7.22 (m, 2H), 7.25-7.29 (m, 1H), 7.37-7.45 (m, 3H), 7.58 (d, *J* = 7.81 Hz, 1H), 7.66 (d, *J* = 8.7 Hz, 1H), 8.91 (t, *J* = 5.0 Hz, 1H); LCMS m/z: 511.28 [M+H]⁺.

4.9 Synthesis of indoles and derivatives

4.9.1 3-Benzyl-N-(furan-2-ylmethyl)-1,3-dimethyl-2-oxoindoline-5-carboxamide (**33**)

To a stirred solution of 3-benzyl-1,3-dimethyl-2-oxoindoline-5-carboxylic acid (120 mg, 0.407 mmol) in DCM (10.0 mL) was added TEA (0.117 mL, 0.813 mmol) and HATU (231 mg, 0.610 mmol) followed by furan-2-ylmethanamine (0.099 mL, 0.447 mmol) dropwise and the whole allowed to stir at RT for 2 h. UPLC and TLC showed formation of the desired compound. The reaction mixture was diluted with water and extracted with EtOAc, the organic layer was washed sequentially with aqueous NaHCO₃ solution, 1N HCl and finally brine, dried over anhydrous Na₂SO₄ and evaporated *in vacuo* to give the crude material which was purified by Combi-flash to afford the title compound **33** (80 mg, 52% yield) as a pale yellow solid. Purity UPLC: 98.30%; ¹H-NMR (500 MHz; DMSO-d₆): δ 1.41 (s, 3H), 2.92 (s, 3H), 3.07 (d, *J* = 4.8 Hz, 2H), 4.48 (d, *J* = 2.8 Hz, 2H), 6.31 (s, 1H), 6.43 (s, 1H), 6.77 (s, 2H), 6.84 (d, *J* = 8.15 Hz, 1H), 7.02 (s, 3H), 7.61 (s, 1H), 7.75 (d, *J* = 8.05 Hz, 1H), 7.97 (s, 1H), 8.86 (t, *J* = 5.2 Hz, 1H); LCMS m/z: 375 [M+H]⁺; HRMS (ESI) m/z: [M+H]⁺ calcd for C₂₃H₂₂N₂O₃ 375.1709, found 375.1703.

4.9.2 1-Benzyl-N-(furan-2-ylmethyl)-1H-indole-6-carboxamide (**34**)

Purity UPLC: 98.78%; ¹H-NMR (500 MHz; DMSO-d₆): δ 4.47 (d, *J* = 5.65 Hz, 2H), 5.49 (s, 2H), 6.26 (d, *J* = 3.0 Hz, 1H), 6.40 (t, *J* = 2.05 Hz, 1H), 6.55 (d, *J* = 3.0 Hz, 1H), 7.18 (d, *J* = 7.5 Hz, 2H), 7.24-7.27 (m, 1H), 7.30-7.33 (m, 2H), 7.58-7.62 (m, 3H), 7.66 (s, 1H), 8.08 (s, 1H), 8.86 (t, *J* = 5.6 Hz, 1H); LCMS m/z: 331 [M+H]⁺; HRMS (ESI) m/z: [M+H]⁺ calcd for C₂₁H₁₈N₂O₂ 331.1447, found 331.1430.

4.9.3 1-(2-Fluorobenzyl)-N-(furan-2-ylmethyl)-3,3-dimethyl-2-oxoindoline-6-carboxamide (**35**)

Purity UPLC: 99.63%; $^1\text{H-NMR}$ (500 MHz; DMSO-d_6): δ 1.36 (s, 6H) 4.45 (d, $J = 5.6$ Hz, 2H), 4.96 (s, 2H), 6.24 (d, $J = 2.85$ Hz, 1H), 6.39 (s, 1H), 7.06-7.12 (m, 3H), 7.37-7.74 (m, 3H), 7.74-7.61 (m, 2H), 8.92 (t, $J = 5.55$ Hz, 1H); LCMS m/z : 393.28 $[\text{M}+\text{H}]^+$; HRMS (ESI) m/z : $[\text{M}+\text{H}]^+$ calcd for $\text{C}_{23}\text{H}_{21}\text{FN}_2\text{O}_3$ 393.1614, found 393.1604.

4.9.4 Synthesis of 1-(2-fluorobenzyl)-3,3-dimethyl-2-oxo-N-(2,4,6-trifluorobenzyl)indoline-6-carboxamide (36)

Purity UPLC: 99.69%; $^1\text{H-NMR}$ (400 MHz; DMSO-d_6): δ 1.33 (s, 6H), 4.41 (d, $J = 4.96$ Hz, 2H), 4.96 (s, 2H), 7.13-7.25 (m, 5H), 7.31-7.31 (m, 2H), 7.46 (d, $J = 7.72$ Hz, 1H), 7.55 (d, $J = 7.24$ Hz, 1H), 8.79 (bs, 1H); LCMS m/z : 457.2 $[\text{M}+\text{H}]^+$; HRMS (ESI) m/z : $[\text{M}+\text{H}]^+$ calcd for $\text{C}_{25}\text{H}_{20}\text{F}_4\text{N}_2\text{O}_2$ 457.1539, found 457.1529.

4.9.5 1-(2-Chloro-6-fluorobenzyl)-3,3-dimethyl-2-oxo-N-(2,4,6-trifluorobenzyl)indoline-6-carboxamide (53)

Purity UPLC: 99.70%; $^1\text{H-NMR}$ (500 MHz; DMSO-d_6): δ 1.28 (s, 6H), 4.42 (d, $J = 4.95$ Hz, 2H), 5.03 (s, 2H), 7.19-7.26 (m, 3H), 7.31 (s, 1H), 7.35-7.44 (m, 3H), 7.50 (d, $J = 7.8$ Hz, 1H), 8.80 (t, $J = 4.95$ Hz, 1H); LCMS m/z : 491.32 $[\text{M}+\text{H}]^+$; HRMS (ESI) m/z : $[\text{M}+\text{H}]^+$ calcd for $\text{C}_{25}\text{H}_{19}\text{ClF}_4\text{N}_2\text{O}_2$ 491.1149, found 491.1146.

4.9.6 1'-(2-Chloro-6-fluorobenzyl)-N-(furan-2-ylmethyl)-2'-oxospiro[cyclopropane-1,3'-indoline]-6'-carboxamide (42)

Purity UPLC: 98.53%; $^1\text{H-NMR}$ (400 MHz; DMSO-d_6): δ 1.58 (s, 2H), 1.69 (s, 2H), 4.43 (d, $J = 4.88$ Hz, 2H), 5.12 (s, 2H), 6.25 (s, 1H), 6.39 (s, 1H), 7.10 (d, $J = 7.68$ Hz, 1H), 7.22 (t, $J = 8.8$

Hz, 1H), 7.34-7.40 (m, 2H), 7.52-7.57 (m, 3H), 8.84 (bs, 1H); LCMS m/z: 425 [M+H]⁺; HRMS (ESI) m/z: [M+H]⁺ calcd for C₂₃H₁₈ClFN₂O₃ 425.1068, found 425.1056.

4.9.7 1-(2-Fluorobenzyl)-N-(furan-2-ylmethyl)-2,3-dioxindoline-6-carboxamide (40)

Purity UPLC: 97.47%; ¹H-NMR (500 MHz; DMSO-d₆): δ 4.44 (d, *J* = 5.5 Hz, 2H), 4.98 (s, 2H), 6.27 (d, *J* = 2.45 Hz, 1H), 6.40 (s, 1H), 7.15 (t, *J* = 7.45 Hz, 1H), 7.25-7.31 (m, 1H), 7.35-7.41 (m, 2H), 7.47-7.50 (m, 1H), 7.60 (d, *J* = 9.35 Hz, 2H), 7.69 (d, *J* = 7.7 Hz, 1H), 9.18 (t, *J* = 5.45 Hz, 1H); LCMS m/z: 377.24 [M-H]⁺; HRMS (ESI) m/z: [M+H]⁺ calcd for C₂₁H₁₅FN₂O₄ 379.1094, found 379.1085.

4.9.8 1-(2-Chloro-6-fluorobenzyl)-3-hydroxy-3-methyl-2-oxo-N-(2,4,6-trifluorobenzyl)indoline-6-carboxamide (39)

Purity UPLC: 97.40%; ¹H-NMR (500 MHz; DMSO-d₆): δ 1.38 (s, 3H), 4.43 (d, *J* = 4.95 Hz, 2H), 4.90 (d, *J* = 15.5 Hz, 1H), 5.11 (d, *J* = 15.4 Hz, 1H), 6.20 (s, 1H), 7.19-7.27 (m, 3H), 7.32-7.43 (m, 4H), 7.50 (d, *J* = 7.75 Hz, 1H), 8.83 (t, *J* = 5.05 Hz, 1H); LCMS m/z: 493.26 [M+H]⁺; HRMS (ESI) m/z: [M+H]⁺ calcd for C₂₄H₁₇ClF₄N₂O₃ 493.0942, found 493.0933.

4.9.9 1-(2-Chloro-6-fluorobenzyl)-3-methoxy-3-methyl-2-oxo-N-(2,4,6-trifluorobenzyl)indoline-6-carboxamide (38)

Purity UPLC: 96.57%; ¹H-NMR (500 MHz; DMSO-d₆): δ 1.41 (s, 3H), 2.86 (s, 3H), 4.42-4.47 (m, 2H), 5.02-5.10 (q, *J*₁ = 15.5 Hz, *J*₂ = 23.45 Hz, 2H), 7.19-7.27 (m, 3H), 7.31-7.44 (m, 4H), 7.57 (d, *J* = 7.65 Hz, 1H), 8.88 (t, *J* = 5.0 Hz, 1H); LCMS m/z: 507.31 [M+H]⁺; HRMS (ESI) m/z: [M+H]⁺ calcd for C₂₅H₁₉ClF₄N₂O₃ 507.1099, found 507.1090.

4.9.10 *1-(2-Chloro-6-fluorobenzyl)-3-cyano-3-methyl-2-oxo-N-(2,4,6-trifluorobenzyl)indoline-6-carboxamide (54)*

Purity UPLC: 98.24%; ¹H-NMR (500 MHz; DMSO-d₆): δ 1.77 (s, 3H), 4.46 (s, 2H), 5.12 (s, 2H), 7.2 (t, *J* = 7.05 Hz, 2H), 7.28 (t, *J* = 8.6 Hz, 1H), 7.38-7.45 (m, 3H), 7.63 (d, *J* = 6.8 Hz, 1H), 7.75 (d, *J* = 7.35 Hz, 1H), 8.90 (bs, 1H); LCMS m/z: 502.12 [M+H]⁺; HRMS (ESI) m/z: [M+H]⁺ calcd for C₂₅H₁₆ClF₄N₃O₂ 502.0945, found 502.0933.

4.9.11 *3-Cyano-1-(3,5-difluorobenzyl)-3-methyl-2-oxo-N-(2,4,6-trifluorobenzyl)indoline-6-carboxamide (55)*

Purity UPLC: 99.19%; ¹H-NMR (500 MHz; DMSO-d₆): δ 1.85 (s, 3H), 4.46 (d, *J* = 5.0 Hz, 2H), 4.97-5.06 (q, *J* = 16.55 Hz, 2H), 7.04 (d, *J* = 6.35 Hz, 2H), 7.16-7.23 (m, 3H), 7.49 (s, 1H), 7.68 (d, *J* = 7.85 Hz, 1H), 7.80 (d, *J* = 7.85 Hz, 1H), 8.97 (t, *J* = 5.1 Hz, 1H); LCMS m/z: 486.33 [M+H]⁺; HRMS (ESI) m/z: [M+H]⁺ calcd for C₂₅H₁₆F₅N₃O₂ 486.1241, found 486.1229.

4.10 *General procedures for synthesis of tetrahydroquinazolinone intermediates*

4.10.1 *Methyl 3-(benzylcarbamoyl)-4-nitrobenzoate*

To a stirred solution of 5-(methoxycarbonyl)-2-nitrobenzoic acid (0.4 g, 1.77 mmol) in DMF (5.0 mL) was added benzylamine (0.231 mL, 2.115 mmol) and HATU (1.01 g, 2.66 mmol), followed by TEA (0.513 mL, 3.5 mmol) dropwise into the solution and the combined mixture was allowed to stir at RT for 1h. UPLC and TLC showed formation of the desired product. The reaction mixture was diluted with water, extracted with EtOAc and the organic layer was washed with 1N HCl and then brine before it was dried over anhydrous Na₂SO₄ and evaporated *in vacuo*

to give the title compound (600 mg) as a crude solid which was used in the next step without any further purification. LCMS m/z: 315 [M+H]⁺.

4.10.2 Methyl 4-amino-3-(benzylcarbamoyl)benzoate

To a stirred solution of methyl 3-(benzylcarbamoyl)-4-nitrobenzoate (600 mg, 1.91 mmol) in a mixture of solvents MeOH (50 mL) and EtOAc (25 mL) was added 10% Pd/C (150 mg, wet) under an inert atmosphere. The whole was stirred under H₂ gas balloon pressure at RT for 1 h. TLC showed complete consumption of starting material, and so the reaction mixture was filtered through a celite bed and the bed was washed with MeOH. The filtrate was evaporated *in vacuo* to afford the title compound (550 mg, crude) as a faint brownish solid which was used in the next step without any further purification. LCMS m/z: 285 [M+H]⁺.

4.10.3 Methyl 3-benzyl-2,4-dioxo-1,2,3,4-tetrahydroquinazoline-6-carboxylate

To a stirred solution of methyl 4-amino-3-(benzylcarbamoyl)benzoate (420 mg, 1.47 mmol) in DCM (1.0 mL) was added triphosgene (877 mg, 2.95 mmol) and the resulting reaction mixture was stirred at RT for 30 minutes. TEA (0.64 mL, 4.434 mmol) was added and the combined mixture was stirred at RT for 1 h. TLC showed complete consumption of the starting material, and so the mixture was diluted with 1N HCl and the organic layer was separated, washed with brine, dried over Na₂SO₄ and evaporated *in vacuo* to give a crude material which was purified by Combi-flash to afford the title compound (161 mg, 35% yield) as an off white solid. LCMS m/z: 311 [M+H]⁺.

4.10.4 3-Benzyl-2,4-dioxo-1,2,3,4-tetrahydroquinazoline-6-carboxylic acid

To a stirred solution of methyl 3-benzyl-2,4-dioxo-1,2,3,4-tetrahydroquinazoline-6-carboxylate (160 mg, 0.516 mmol) in a mixture of THF (10 mL) and water (5 mL) was added LiOH.H₂O (43 mg, 1.08 mmol) at RT and the resulting reaction mixture was stirred at RT for 1 h. TLC showed complete consumption of the starting material, and so the solvents were evaporated and the crude product was washed with ether, the aqueous layer was acidified with 1N HCl, and the precipitate was filtered and washed with water and dried in a vacuum oven to afford the title compound (100 mg, 65% yield) as an off-white solid. LCMS m/z: 297 [M+H]⁺.

4.11 Synthesis of tetrahydroquinazolinones

4.11.1 3-Benzyl-N-(furan-2-ylmethyl)-2,4-dioxo-1,2,3,4-tetrahydroquinazoline-6-carboxamide (37)

To a stirred solution of 3-benzyl-2,4-dioxo-1,2,3,4-tetrahydroquinazoline-6-carboxylic acid (100 mg, 0.337 mmol) in DCM (10.0 mL) was added furan-2-ylmethanamine (0.032 mL, 0.37 mmol) and HATU (192 mg, 0.506 mmol), followed by TEA (0.097 mL, 0.674 mmol) dropwise into the solution and the combined mixture was allowed to stir at RT for 2 h. UPLC and TLC showed formation of the desired product and upon completion the reaction mixture was diluted with water and extracted with EtOAc, the organic layer was washed sequentially with aqueous NaHCO₃ solution, 1N HCl and finally with brine, dried over anhydrous Na₂SO₄ and evaporated *in vacuo* to give the crude product which was purified by Combi-flash to afford the title compound **37** (104 mg, 82% yield) as a pale yellow solid. Purity UPLC: 98.07%; ¹H-NMR (500 MHz; DMSO-d₆): δ 4.46 (d, *J* = 5.5 Hz, 2H), 5.11 (s, 2H), 6.28 (d, *J* = 2.9 Hz, 1H), 6.40 (s, 1H), 7.24 (d, *J* = 8.5 Hz, 2H), 7.29-7.32 (m, 4H), 7.59 (s, 1H), 8.16 (d, *J* = 8.5 Hz, 1H), 8.53 (s, 1H),

9.18 (t, $J = 5.45$ Hz, 1H), 11.80 (s, 1H); LCMS m/z: 376 [M+H]⁺; HRMS (ESI) m/z: [M+H]⁺ calcd for C₂₁H₁₇N₃O₄ 376.1297, found 376.1288.

4.12 General procedures for synthesis of benzimidazolinone intermediates

4.12.1 Methyl 3-bromo-4-((ethoxycarbonyl)amino)benzoate

To a stirred solution of commercially available methyl 4-amino-3-bromobenzoate (1.1 g, 4.808 mmol) in pyridine (10 mL) was added ethyl chloroformate (0.45 mL, 4.808 mmol) at 0-5 °C and the resulting reaction mixture was stirred at 0-5 °C for 1 h. TLC and LCMS showed formation of the desired compound and so the reaction mixture was quenched with ice cold water. The precipitated solid was filtered, washed with water and then dried in a vacuum oven to afford the title compound (760 mg, 52% yield) as an off white solid. LCMS m/z: 301 [M+H]⁺.

4.12.2 Methyl 3-(2-chlorobenzyl)-2-oxo-2,3-dihydro-1H-benzo[d]imidazole-5-carboxylate

To a stirred solution of methyl 3-bromo-4-((ethoxycarbonyl)amino)benzoate (760 mg, 2.533 mmol) in DMSO (10 mL) was added CuI (96 mg, 0.506 mmol), 4-hydroxy *trans*-L-proline (132 mg, 1.013 mmol), K₃PO₄ (1.075 mg, 5.066 mmol) and 2-chloro-benzyl amine (0.305 mL, 2.533 mmol). The resulting reaction mixture was stirred at 70-75 °C for 16 h. TLC and LCMS showed formation of the desired compound along with some un-cyclized intermediate. Stirring was therefore continued at 90-95 °C for 5 h and after completion the reaction mixture was quenched with ice cold water and extracted with EtOAc. The combined organic layers were washed with brine, dried over anhydrous Na₂SO₄ and evaporated *in vacuo* to afford the crude product which was purified by Combi-flash to give the title compound (210 mg, 26% yield) as a pale yellow solid. LCMS m/z: 317 [M+H]⁺.

4.12.3 3-(2-Chlorobenzyl)-2-oxo-2,3-dihydro-1H-benzo[d]imidazole-5-carboxylic acid

A solution of methyl 3-(2-chlorobenzyl)-2-oxo-2,3-dihydro-1H-benzo[d]imidazole-5-carboxylate (110 mg, 0.348 mmol) in a mixture of AcOH (1.5 mL) and HCl (1.5 mL) was stirred at 80 °C for 5 h. TLC and LCMS showed formation of the desired compound. The reaction mixture was cooled to RT to give a solid precipitate which was filtered, washed with water and dried in a vacuum oven to afford the title compound (90 mg, 86% yield) as a gray solid. LCMS m/z: 303 [M+H]⁺.

4.13 Synthesis of benzimidazolinones

4.13.1 3-(2-Chlorobenzyl)-N-(furan-2-ylmethyl)-2-oxo-2,3-dihydro-1H-benzo[d]imidazole-5-carboxamide (**41**)

To a stirred solution of 3-(2-chlorobenzyl)-2-oxo-2,3-dihydro-1H-benzo[d]imidazole-5-carboxylic acid (100 mg, 0.331 mmol) in DCM (5 mL) was added TEA (0.0955 mL, 0.6622 mmol), HATU (188 mg, 0.496 mmol) and furan-2-ylmethanamine (0.032 mL, 0.364 mmol) dropwise into the solution and the whole was allowed to stir at RT for 1 h. Progress of the reaction was monitored by UPLC and TLC and after completion the reaction mixture was diluted with water and extracted with EtOAc. The combined organic layers were washed with aqueous NaHCO₃ solution, 1N HCl and finally with brine, dried over anhydrous Na₂SO₄ and evaporated *in vacuo* to give the crude product which was purified by Combi-flash to afford the title compound **41** (80 mg, 63% yield) as a pale brown solid. Purity UPLC: 98.37%; ¹H-NMR (500 MHz; DMSO-d₆): δ 4.42 (s, 2H), 5.11 (s, 2H), 5.77 (s, 1H), 6.23 (s, 1H), 6.38 (s, 1H), 6.91 (s,

1H), 7.11 (s, 1H), 7.28-7.34 (m, 2H), 7.54-7.65 (m, 3H), 8.72 (s, 1H), 11.38 (s, 1H); LCMS m/z: 382 [M+H]⁺; HRMS (ESI) m/z: [M+H]⁺ calcd for C₂₀H₁₆ClN₃O₃ 382.0958, found 382.0946.

4.14 Cell lines

Stable HEK293T STING-expressing cell lines were generated using plasmids purchased from Invivogen, CA, USA, that contain STING cDNA cloned into the pUNO-1 vector under hEF1-HTLV promoter and containing the Blasticidin selection cassette. The plasmids hSTING (R232), hSTING (H232), hSTING (HAQ) were directly procured from Invivogen while hSTING (AQ) and hSTING (Q) were derived from hSTING (HAQ) and hSTING (R232) plasmids respectively by using a PCR based site directed mutagenesis method. These vectors were individually transfected into HEK293T cells using Lipofectamine (Invitrogen) and transfected cells were selected under Blasticidin selection. These transfected cells were further subjected to clonal selection using the limiting dilution method to obtain clonally pure populations of HEK cells transfected with each of the above mentioned human STING variants. Only those clones were selected in which ligand independent activation of STING was minimal. Stable HEK293T Luciferase reporter gene expressing cell lines were generated using pCDNA4 plasmids under an IRF-inducible promoter using similar methods.

4.15 Luciferase Assay

5 x 10⁵ clonally selected HEK293T-hSTING-Luciferase cells or control HEK293T-Luciferase cells were seeded in 384-well plates in growth medium and stimulated with known STING agonists or novel compounds. Supernatants were removed after 20 hours of treatment and

secretory reporter gene activity was measured using the Quanti-Luc detection system (Invivogen) on a Spectramax i3X luminometer.

4.16 Western blot assay

5×10^5 cells were seeded in 24-well plates in 500 μ l growth medium and stimulated with novel compounds at 10 μ M. After 2 hours of treatment cells were harvested by centrifugation and cell pellets were lysed in RIPA buffer (20mM Tris-Cl, 150mM NaCl, 0.5mM EDTA, 1% NP40, 0.05% SDS) containing 1x phosphatase inhibitor cocktail 3 (Sigma) and 1x protease inhibitor (Roche) to extract the soluble fraction of protein. 10 μ g of extracted protein was electrophoresed in 10% SDS-PAGE gels and transferred onto Immobilon-P membranes (Millipore). Blots were incubated with antibodies specific for phosphorylated STING (Ser366), phosphorylated IRF3 (Ser396), total STING, Actin (Cell Signaling) and IRF3 (Abcam). Anti-rabbit HRP label secondary antibody (Abcam) and Clarity MaxTM western ECL substrate (Biorad - cat# 1705062) were used for visualization of bands using a BioRad XRS *plus* imager.

4.17 In vitro kinase assay

50ng of recombinant STING protein (Cayman Chemicals Cat# 22816) corresponding to the soluble domain of STING (138 to 379 aa) protein or 1 μ l of ER fraction (8mg/ml) containing full length STING from R232.hSTING was incubated with 20 ng of recombinant full length TBK1 protein (Invitrogen, Cat# A31514) in the presence/absence of test compound in 20 μ l reaction buffer (50mM Tris-HCl of pH 7.4, 100mM NaCl, 5mM MgCl₂, 5mM MnCl₂, 10% glycerol, 0.2mM Na₃VO₄, 20mM β -glycero-PO₄, 0.5mM ATP) and 0.01% BSA at 30 °C for 45 min. The reaction was quenched by addition of 2 μ l of 10X EDTA to a final concentration of 50 μ M.

Samples were treated with 4x gel loading dye followed by electrophoresis in 10% SDS-PAGE gels and transferred to Immobilon-P membranes (Millipore). Blots were incubated with antibodies specific for phosphorylated STING (Ser366) and total STING (Cell Signaling). Anti-rabbit HRP labelled secondary antibody (Abcam) and Clarity MaxTM western ECL substrate (Biorad, Cat# 1705062) were used for visualization of bands using a BioRad XRS *plus* imager.

4.18 qRT-PCR Analysis of Cytokines

Freshly isolated 2×10^5 human PBMCs using Histopaque (Sigma) of different healthy donors were stimulated with compound 53 in 200 μ l growth medium at 6 hr (early) or 20h (late) for cytokine induction. Post treatment cells were harvested through centrifugation and the cell pellets were used to isolate total RNA using the Nucleospin RNA plus kit (Macherey-Nagel). Total RNA was quantified by Quanti fluor RNA system kit (Promega) and an equal amount of RNA was used to synthesize cDNA using Maxima Reverse transcriptase (Thermo). Expression of respective genes was measured by real-time qRT-PCR using an equal amount of cDNA (quantified by Quanti fluor RNA system kit) of each treatment and specific primers for human IFN α , β , TNF α , CXCL10, IL12p40, IL1 β , CCL20, IL4, IFN γ & IL6. The real time PCR reactions were performed using BioRad CFX-96 and Sso advanced universal SYBR green supermix (BioRad). Data was analyzed as relative fold of expression with respect to vehicle treatment.

4.19 DC maturation & Activation assay

Freshly isolated 5×10^7 PBMC from human whole blood using a polysucrose gradient 1.077g/ml (Histopaque 1077, Sigma) followed by ACK lysis and subsequent wash were used to

isolate human monocytes as per MACS monocyte isolation kit (Cat# 130-050-201). Monocytes were resuspended in Complete growth medium (RPMI + 10% Heat inactivated FBS + 2mM Glutamine + 50uM b-ME + 50U/ml Pen-Strep) containing 100ng/ml GMCSF and 50ng/ml IL4 at a density of 1×10^6 cells/ml and plated in a 48-well TC plate in 300ul volume followed by incubation at 37°C humidified 5% CO₂ tissue incubator. After 24 h to 36 h incubation, compound 53 or the corresponding vehicle (1% DMSO final) was added to the respective wells and further incubated for another 6 h. Following compound treatment cells were harvested and cell pellets were used to monitor for DC activation markers (CD86 & CD83) as well as cytokines (IFN α , IFN β , TNF α , IL6, IL12p40, CXCL10) induction at 6h by qPCR.

4.20 Pharmacokinetics

Pharmacokinetic (PK) studies were conducted in Balb/c mice according to the protocol approved by the Institutional Animal Ethics Committee (IAEC). Briefly compound was dissolved in DMA by vortexing and then required volumes of PEG, PG and saline were added sequentially (with vortexing) to obtain a clear solution for dosing. Overnight fasted mice were randomized into different groups (n=3/group). Mice received a single intravenous or oral dose of the compound (lateral tail vein or oral gavage). The blood samples were collected through retro-orbital plexus at different time points after dosing (50 μ l/ time point, under isoflurane anesthesia). Blood samples were collected at 2 min, 10 min, 30 min, 1 h, 2 h, 4 h, 6 h, 8 h & 24 h after intravenous dosing whereas at 5 min, 15 min, 30 min, 1 h, 2 h, 4 h, 6 h, 8 h & 24 h after oral dosing. Blood samples were centrifuged at 1500 x g for 15 min at 4 °C; plasma samples were separated and stored at -80 °C until subjected to LCMS analysis.

Author contributions

The manuscript was written through contributions of all authors. All authors have given approval to the final version of the manuscript.

Acknowledgements

The authors thank Dr. Paul Greenspan and Dr. Stepan Vyskocil of Takeda Pharmaceuticals for providing a critical review of the manuscript.

The authors would like to thank the following scientists from Curadev for excellent technical support: Thanilsana Soram, Kavita Puniya, Priti Sharma, Ritika Raina, Debjani Chakraborty, Abhisek Chatterjee, Rubeenaparveen Rais Mansuri, Anuj Singh. The authors also thank TCG Lifesciences, Kolkata for synthesis and compound characterisation support.

Supporting Material.

Supporting Material for this article can be found online at <https://doi.org/XXXXXXXXXX>

Abbreviations

AcOH, acetic acid; MeCN, acetonitrile; MeOH, methanol; TEA, triethylamine; DIPEA, diisopropylethylamine; HATU, 1-[bis(dimethylamino)methylene]-1*H*-1,2,3-triazolo[4,5-*b*]pyridinium-3-oxide hexafluorophosphate; HBTU, *N,N,N',N'*-tetramethyl-*O*-(1*H*-benzotriazol-1-yl)uronium hexafluorophosphate; HOBt, 1-hydroxybenzotriazole; THF, tetrahydrofuran; DMA, dimethylacetamide; DMF, dimethylformamide; DCM, dichloromethane; DBU, 1,8-diazabicyclo[5.4.0]undec-7-ene; PEG, polyethylene glycol; PG, propylene glycol; NS, normal

saline; TLC, thin layer chromatography; EDC, N-(3-Dimethylaminopropyl)-N'-ethylcarbodiimide; TBAB, *tetra n*-butylammonium bromide; RT, room temperature; mCPBA, meta-chloro perbenzoic acid; MTBE, methyl *tert*-butyl ether; T3P, propanephosphonic acid anhydride; LCMS, liquid chromatography-mass spectrometry; HPLC/UPLC high performance liquid chromatography/ultra performance liquid chromatography.

Journal Pre-proof

References

- [1] Oiseth, S. J. and Aziz, M. S., Cancer immunotherapy: a brief review of the history, possibilities, and challenges ahead, *J. Cancer Metastasis Treat.* 3 (2017) 250-261.
- [2] Weinmann, H., Cancer immunotherapy: selected targets and small-molecule modulators, *ChemMedChem* 11 (2016) 450-466.
- [3] Kawai, T. and Akira, S., Antiviral signaling through pattern recognition receptors, *J. Biochem.* 141 (2006) 137-145.
- [4] Silva-Gomes, S.; Decout, A.; Nigou, J., 2014, Pathogen-Associated Molecular Patterns (PAMPs). In: Parnham, M. (eds) *Encyclopedia of Inflammatory Diseases*. Birkhäuser, Basel.
- [5] a) Horscroft, N. J., Pryde, D. C.; Bright, H., Antiviral applications of Toll-like receptors, *J. Antimicrob. Ther.* 67 (2012) 789-801. b) Diebold, S. S.; Kaisho, T.; Hemmi, H.; Akira, S.; Reis e Sousa, C., Innate antiviral responses by means of TLR7-mediated recognition of single-stranded RNA, *Science* 303 (2004) 1529-1531.
- [6] Pichlmair, A.; Schulz, O.; Ping Tan, C.; Naslund, T. I.; Liljestrom, P.; Weber, F.; Reis e Sousa, C., RIG-I mediated antiviral responses to single-stranded RNA bearing 5'-phosphates, *Science*, 314 (2006) 997-1001.
- [7] Takeuchi, O. and Akira, S., Pattern recognition receptors and inflammation, *Cell* 140 (2010) 805-820.
- [8] a) Ishikawa, H and Barber, G., STING is an endoplasmic reticulum adaptor that facilitates innate immune signaling, *Nature* 455 (2008) 674-678. b) Burdette, D. L. and Vance, R. E., *Nat. Immunol.* 14 (2013) 19-26.

- [9] Zhang, X., Shi, H., Wu, J., Zhang, X., Sun, L., Chen, C. and Chen, Z.J., Cyclic GMP-AMP containing mixed phosphodiester linkages is an endogenous high-affinity ligand for STING, *Mol. Cell* 51, (2013) 226-235.
- [10] a) Burdette, D. L.; Monroe, K. M.; Sotelo-Troha, K.; Iwig, J. S.; Eckert, B.; Hyodo, M.; Hayakawa, Y.; Vance, R. E., STING is a direct innate immune sensor of cyclic di-GMP, *Nature* 478 (2011) 515-518. b) DeFilippis, V. R.; Alvarado, D.; Sali, T.; Rothenburg, S.; Fruh, K., Human cytomegalovirus induces the interferon response via the DNA sensor ZBP1, *J. Virol.* 84 (2010) 585-598.
- [11] Woo, S-R.; Corrales, L.; Gajewski, T. F., Innate immune recognition of cancer, *Annu. Rev. Immunol.* 33 (2015) 445-474.
- [12] Baguley, B. C. and Ching, L. M., DMXAA: an antivasular agent with multiple host responses, *Int. J. Radiat. Oncol. Biol. Phys.* 54 (2002) 1503-1511.
- [13] a) Lara, P. N.; Douillard, J-Y.; Nakagawa, K.; von Pawel, J.; McKeage, M. J.; Albert, I.; Losonczy, G.; Reck, M.; Heo, D-S.; Fan, X.; Fandi, A.; Scagliotti, G., Randomized phase III placebo-controlled trial of carboplatin and paclitaxel with or without the vascular disrupting agent vadimezan (ASA404) in advanced non-small-cell lung cancer, *J. Clin. Oncol.* 29 (2011) 2965-2971. b) Conlon, J.; Burdette, D. L.; Sharma, S.; Bhat, N.; Thompson, M.; Jiang, Z.; Rathinam, V. A. K.; Monks, B.; Jin, T.; Xiao, T. S.; Vogel, S. N.; Vance, R. E.; Fitzgerald, K. A., Mouse, but not human, STING binds and signals in response to the vascular disrupting agent 5,6-dimethylxanthenone-4-acetic acid, *J. Immunol.* 190 (2013) 5216-5225.
- [14] a) Cavlar, T.; Deimling, T.; Ablasser, A.; Hopfner, K-P.; Hornung, V., Species-specific detection of the antiviral small-molecule compound CMA by STING, *EMBO J.* 32 (2013)

1440-1450. b) Kim, S.; Li, L.; Maliga, Z.; Yin, Q.; Wu, H.; Mitchison, T.J., Anticancer flavonoids are mouse-selective STING agonists, *ACS Chem. Biol.* 8 (2013) 1396-1401.

[15] a) Corrales, L.; Glickman, L. H.; McWhirter, S. M.; Kanne, D. B.; Sivick, K. E.; Katibah, G. E.; Woo, S. R.; Lemmens, E.; Banda, T.; Leong, J. J.; Metchette, K.; Dubensky, T. W. Jr.; Gajewski, T. F., Direct activation of STING in the tumor microenvironment leads to potent and systemic tumor regression and immunity, *Cell Rep.* 11 (2015) 1018-1030. b) Aduro Biotech, <http://www.aduro.com/pipeline/clinical-trials> (accessed November 29, 2019). c) Clinical Trials .gov, <http://clinicaltrials.gov/ct2/show/NCT03172936> (accessed November 29, 2019). d) Clinical Trials .gov, <http://clinicaltrials.gov/ct2/show/NCT02675439> (accessed November 29, 2019). e) Aduro Biotech, <http://investors.aduro.com/phoenix.zhtml?c=242043&p=irol-newsArticle&ID=2376492> (accessed November 29, 2019).

[16] a) Clinical Trials .gov, <http://clinicaltrials.gov/ct2/show/NCT03010176> (accessed November 29, 2019). b) Business Wire, <https://www.businesswire.com/news/home/20181020005008/en/Presentation-Early-Data-Merck%E2%80%99s-Investigational-STING-Agonist> (accessed November 29, 2019).

[17] a) Yan, H.; Wang, X.; KuoLee, R.; Chen, W., Synthesis and immunostimulatory properties of the phosphorothioate analogues of cdiGMP, *Bioorg. Med. Chem. Letts.* 18 (2008) 5631-5634. b) Li, L.; Yin, Q.; Kuss, P.; Maliga, Z.; Millan, J. L.; Wu, H.; Mitchison, T. J., Hydrolysis of 2',3'-cGAMP by ENPP1 and design of nonhydrolyzable analogs, *Nat. Chem. Biol.* 10 (2014) 1043-1048. c) Dubensky, T.W., Leong, M.L.L., Pardoll, D.M., Kim, Y.J., Compositions and methods for cancer immunotherapy, PCT WO2013185052, 2013. d) Biggadike, K., Champigny, A.C., Coe, D.M., Needham, D., Tape, D.T., Cyclic di-nucleotides

as modulators of STING, PCT WO2015185565, 2015. e) Altman, M.D., Andresen, B., Chang, W., Childers, M.L., Cumming, J.N., Haidle, A.M., Henderson, T.J., Jewell, J.P., Liang, R., Lim, J., Liu, H., Lu, M., Northrup, A.B., Otte, R.D., Siu, T., Trotter, B.W., Truong, Q.T., Walsh, S.P., Zhao, K., Cyclic di-nucleotide compounds as STING agonists, PCT WO2017027646, 2017. f) Glick, G., Ghosh, S., Roush, W.R., Olhava, E.J., Jones, R., Cyclic dinucleotide analogs for treating conditions associated with STING (Stimulator of Interferon genes) activity, PCT WO2018045204, 2018. g) Iyer, R.P., Coughlin, J.E., Design of oligonucleotide analogs as therapeutic agents, US Patent US20150329864, 2015.

[18] a) Kimura, Y.; Negishi, H.; Matsuda, A.; Endo, N.; Hangai, S.; Inoue, A.; Nishio, J.; Taniguchi, T.; Yanai, H. *Cancer Sci.* 109 (2018), 2687-2696. b) Zhang, Y.; Sun, Z.; Pei, J.; Luo, Q.; Zeng, X.; Li, Q.; Yang, Z.; Quan, J., Identification of alpha-mangostin as an agonist of human STING, *ChemMedChem* 13 (2018) 2057-2064. c) Gall, B.; Pryke, K.; Abraham, J.; Mizuno, N.; Botto, S.; Sali, T. M.; Broeckel, R.; Haese, N.; Nilsen, A.; Placzek, A.; Morrison, T.; Heise, M.; Streblow, D.; DeFilippis, V., Emerging alphaviruses are sensitive to cellular states induced by a novel small-molecule agonist of the STING pathway, *J. Virol.* 92 (2018) e01913-17. d) Liu, B.; Tang, L.; Zhang, X.; Ma, J.; Sehgal, M.; Cheng, J.; Zhang, X.; Zhou, Y.; Du, Y.; Kulp, J.; Guo, J.; Chang, J., A cell-based high throughput screening assay for the discovery of cGAS-STING pathway agonists, *Antiviral Res.*, 147 (2017) 37-46.

[19] Wu, J. H., Tian, X. Compounds and uses thereof in the treatment of cancers and other medical conditions., PCT WO2017011920, 2017.

[20] Altman, M.D., Cash, B.D., Chang, W., Cumming, J.N., Haidle, A.M., Henderson, T.J., Jewell, J.P., Larsen, M.A., Liang, R., Lim, J., Lu, M., Otte, R.D., Siu, T., Trotter, B.W.,

Tyagarajan, S. Benzo[*b*]thiophene compounds as STING agonists. Merck Sharp and Dohme Corp., PCT WO2018067423, 2018.

[21] Ramanjulu, J. M., Pesiridis, G. S., Yang, J., Concha, N. O., Singhaus, R., Zhang, S., Tran, J., Moore, P., Lehmann, S., Eberl, H. C., Muelbaier, M., Schneck, J., Clemens, J., Adam, M., Mehlman, J., Romano, J., Morales, A., Kang, J., Leister, L., Charnley, A., Hughes, T., Ye, G., Nevins, N., Behnia, K., Wolf, A., Kasparcova, V., Nurse, K., Wang, L., Li, Y., Klein, M., Hopson, C., Guss, J., Bantscheff, M., Bergamini, G., Reilly, M., Lian, Y., Duffy, K., Adams, J., Gough, P. J., Marquis, R., Smother, J., Hoos, A., Bertin, J. J., Design of amidobenzimidazole STING receptor agonists with systemic activity, *Nature* 564 (2018) 439-443.

[22] Gao, P.; Ascano, M.; Zillinger, T.; Wang, W.; Dai, P.; Serganov, A. A.; Gaffney, B. L.; Shuman, S.; Jones, R. A.; Deng, L.; Hartmann, G.; Barchet, W.; Tuschl, T.; Patel, D. J., Structure-function analysis of STING activation by c[G(2',5')pA(3',5')p] *Cell* 154 (2013) 748-762.

[23] Zhang, C.; Shang, G.; Gui, X.; Zhang, X.; Bai, X.; Chen, Z., Structural basis of STING binding with and phosphorylation by TBK1, *Nature* 567 (2019) 394-398.

[24] Diner, E. J.; Burdette, D. L.; Wilson, S. C.; Monroe, K. M.; Kellenberger, C. A.; Hyodo, M.; Hayakawa, Y.; Hammond, M. C.; Vance, R. E., The innate immune DNA sensor cGAS produces a noncanonical cyclic dinucleotide that activates human STING, *Cell Reports* 3 (2013) 1355-1361.

- [25] Yi, G.; Brendel, V. P.; Shu, C.; Li, P.; Palanathan, S.; Kao, C. C., Single nucleotide polymorphisms of human STING can affect innate immune response to cyclic dinucleotides PLoS ONE 8 (2013) e77846.
- [26] Sali, T. M.; Pryke, K. M.; Abraham, J.; Liu, A.; Archer, I.; Broeckel, R.; Stavensky, J. A.; Smith, J. L.; Al-Shammari, A.; Amsler, L.; Sheridan, K.; Nilsen, A.; Streblow, D. N.; DeFillippis, V. R., Characterization of a novel human-specific STING agonist that elicits antiviral activity against emerging alphaviruses, PLoS Pathog. 11 (2015) e1005324.
- [27] Banerjee, M.; Middy, S.; Shrivastava, R.; Basu, S.; Ghosh, R.; Pryde, D.C.; Yadav, D.B.; Surya, A., G10 is a direct activator of human STING, PLoS ONE 15 (2020) e0237743.
- [28] UniProt database. https://www.uniprot.org/uniref/UniRef90_Q86WV6 (accessed December 2nd, 2019).

The Discovery of Potent Small Molecule

Activators of Human STING

*David C. Pryde**, Sandip Middy, Monali Banerjee, Ritesh Shrivastava, Sourav Basu, Rajib Ghosh, Dharmendra B. Yadav, Arjun Surya

Highlights

- Small molecule heterocyclic amides are potent activators of human STING
- Examples of the series directly activate the STING protein
- Examples of the series activate all major polymorphs of human STING
- STING activation with an example compound leads to significant cytokine induction

Declaration of interests

The authors declare that they have no known competing financial interests or personal relationships that could have appeared to influence the work reported in this paper.

The authors declare the following financial interests/personal relationships which may be considered as potential competing interests:

All authors are employees of Curadev Pharma.